

Cover page
Thesis written in
English language.

POLITECNICO DI MILANO

Scuola di Ingegneria Civile, Ambientale e Territoriale



POLO TERRITORIALE DI COMO

Master of Science in

Environmental and Land Planning Engineering

GPR INVESTIGATION AT SAINT ADRIANO CHURCH, BRENNA (CO)

Supervisor: Prof. GIANCARLO BERNASCONI

**Master Graduation Thesis by:
SLOBODAN MILJATOVIC**

Student Id. Number: 765131

Academic Year 2012/2013

First page
Thesis written in
English language.

POLITECNICO DI MILANO

Scuola di Ingegneria Civile, Ambientale e Territoriale



POLO TERRITORIALE DI COMO

**Corso di Laurea Specialistica in
Ingegneria per l'Ambiente e il Territorio**

GPR INVESTIGATION AT SAINT ADRIANO CHURCH, BRENNNA (CO)

Relatore: Prof. GIANCARLO BERNASCONI

**Tesi di Laurea Magistrale di:
SLOBODAN MILJATOVIC**

Matricola: 765131

Anno Accademico 2012/2013

ABSTRACT

Ground Penetrating Radar (GPR) is a geophysical technique used mainly for shallow acquisition and works on the basis of sending electromagnetic waves vertically down to the ground, detecting the response. Data are usually affected by instrumental and environmental noise. The work presented in this master thesis aims to illustrate the processing steps done on the data acquired at the Saint Adriano Roman church in Brenna, Como. The acquisition was conducted in order to try to detect certain ancient structures, such as ancient oratorio, Roman road and graveyard. Initially, random acquisition was done on the site in order to detect areas of interest where more detailed acquisition will be conducted. Three areas are chosen and afterwards, data were recorded and processed using 2D module of REFLEX and after interpreted using 3D module, to provide better understanding of a certain subsurface anomalies.

ACKNOWLEDGEMENTS

At this point I can make a conclusion that past two years spent at Politecnico have substantially enriched my knowledge in both academic and social terms and have completely changed my perception of life. I had an excellent opportunity to experience Italian culture and way of life and at the same time unique international atmosphere in Como Campus. Most of the things I have learned came from some amazing people I have met, both during ASP courses and during my Master course. Thank you very much for everything and a special thank to Politecnico di Milano and Alta Scuola Politecnica for all the support they have provided to us.

My first contact with Geophysics was in the second semester, where I first met professor Bernasconi. Geophysics (and especially GPR) is a unique discipline which allows us to combine history and archeology with technical knowledge, to be able to generate good results. I was very amazed both by the professor's way of teaching and the subject itself, and I have asked him for a project. I would like to thank professor Bernasconi for all the knowledge he has transferred to me, all the support, advices and help. They were much more than essential, thank you professor.

I would like to thank to Dino Ballabio, whose love to history and his place of origin has contributed enormously to the project. I can say that with his knowledge of history of Como and Brenna it was not hard to conduct the research. He is a real example how each of us should love his own place. Thanks for all car rides from Como to Brenna and especially for pizzocheri.

I want to thank my family for unselfish and unconditional support throughout all my life, especially for the support of my father Lazo. Suzana thanks for all the unselfish support in these two years, it meant a lot to me. Special thanks to my friends Putra Dwipa, Simone Frassi, Ahmed Mansi for always useful advices and logistics. I am more than grateful to all of my other friends from Italy, Serbia, Iran, Egypt, Bulgaria, Canada, India, Ethiopia, Macedonia, Brasil, Turkey, Argentina, China and Vietnam for all amazing time we spent together.

CONTENTS

1. INTRODUCTION	11
1.1 BACKGROUND	11
1.2 GROUND PENETRATING RADAR.....	11
1.3 PROBLEM STATEMENT	12
1.4 THESIS OBJECTIVES	13
2. GPR FRAMEWORK	15
2.1 HISTORY OF GPR APPLICATION	15
2.2 THE PHYSICS OF ELECTROMAGNETIC WAVES	16
2.3 INTERACTION WITH THE SUBSURFACE MATERIALS	18
2.3.1 Reflection.....	21
2.3.2 Refraction	21
2.3.3 Diffraction.....	22
2.3.4 Scatter and focusing	22
2.3.5 Dispersion, dissipation and attenuation.....	23
2.3.6 Multiples, ringing, and reverberation.....	23
2.3.7 Background Noise and Clutter.....	23
2.3.8 Attenuation.....	24
2.4 AMPLITUDE ANALYSIS	25
2.4.1 Metals.....	26
2.4.2 Point-Source Reflections	27
2.4.3 Planar Reflections	28
2.5. DEPTH DETERMINATION	29
2.6 GPR IN ARCHEOLOGY	30
3. FUNDAMENTALS OF GPR DATA PROCESSING	34
3.1 DATA EDITING.....	35
3.2 BASIC PROCESSING	35
3.2.1 Dewow	36
3.2.2 Time gain	37
3.2.3 Temporal and spatial filtering	38
3.3 ADVANCED DATA PROCESSING	40
3.3.1 Background Subtraction	40
3.3.2 Deconvolution	41

3.3.3 Migration	42
3.3.4 Attributes	43
3.4 DATA VISUALIZATON	44
3.4.1 Volume visualization.....	45
4. GPR APPLICATIONS TO BURIED ARCHEOLOGICAL FEATURES - CASE STUDIES.....	47
4.1 A GPR SURVEY FOR ARCHEOLOGICAL INVESTIGATIONS IN AN URBAN AREA, LECCE, ITALY	47
4.2 APPLICATION OF GPR IN DETECTING ARCHEOLOGICAL REMAINS IN BUYUK MENDERES GRABEN, TURKEY	51
5. SITE DESCRIPTION AND HISTORY.....	56
6. GPR INVESTIGATION	61
6.1 INSTRUMENTATION.....	61
6.2 ACQUISITION	62
7. RESULTS AND DISCUSSION	66
7.1 THE ROAD	67
7.2 CEMETERY	69
7.3 THE HILL	72
8. CONCLUSIONS AND RECOMMENDATIONS	76
8.1 CONCLUSIONS	76
8.2 RECOMMENDATIONS	77
TABLE OF FIGURES.....	79
TABLES	82
REFERENCES.....	84

1. INTRODUCTION

1.1 BACKGROUND

In the broadest sense, the science of *Geophysics* is the application of physics to investigation of the Earth, Moon and planets. This term can be possibly misleading, so the term Applied Geophysics is usually used for investigation of Earth's crust and near-surface to achieve practical and in many cases economical aim (mainly oil and mineral exploration). Inside this discipline, three sub-disciplines might be identified: archaeo-geophysics, hydro-geophysics and glacio-geophysics. Sometimes it is hard to distinguish them and in many cases they tend to overlap each other. The last method is the least known today although it exists for much longer time than the other two. The various geophysical methods rely on different physical properties of the material (soil) and it is important that the appropriate technique is used for a given type of application. [8]

All geophysical techniques involve indirect measurements of earth related physical attributes and in the case of archaeological structures, contrasts resulting from subsurface disturbances associated with past cultural activities. Most dispersed geophysical methods in this area are: resistivity, high frequency seismic sounding, microgravity, magnetometry and Ground Penetrating Radar (GPR). Mainly due to their preciseness, constantly decreasing costs and non invasive nature, using of geophysical methods have become essential part of modern archeology. [9]

1.2 GROUND PENETRATING RADAR

The term "radar" stands for Radio Detection and Ranging, with the final aim of detecting objects and their properties (position, shape, material, speed etc.) at a certain distance. "Radar" used in geophysical methods is usually referred as a Ground Penetrating Radar, which is the general term applied to geophysical techniques which employ radio waves, typically in the 1 to 1000 MHz

frequency range. GPR has been developed over the past three decades for shallow, high resolution investigations of the subsurface. [13]

The way of operation of the GPR is very similar to the conventional radar systems, meaning that it sends pulses of electromagnetic (EM) waves into the ground. The first aim is to detect the difference among the physical properties of the subsurface features and surrounding material, in order to map structure and features buried in the ground (their shapes, sizes). Afterwards, GPR uses the principle of scattering of electromagnetic waves to locate buried objects. Historically, GPR was primarily focused on mapping structures in the ground and in the last decades GPR has been used also in non-destructive testing of non-metallic structures. [10]

1.3 PROBLEM STATEMENT

Over the past two decades GPR has been regularly applied in archeological application due to its non-invasive nature and soon could become standard procedure prior to archeological field work. Although precise maps could be obtained in some cases, most historical features could be hard to locate in present due to landscape change. Without GPR application, archeologist could face great expenditures for excavation and even risk to fail. In case of Brenna, landscape has been substantially changed and initially it was not clear where the features might be located. About some features such as oratorio no historical evidences have been found except the claims of a certain groups of historians. In practice, using conventional archeological methods the object would be practically impossible to locate. The only historical evidence at the moment is the location of the old Roman road and its location could be anticipated. No historical evidences have been found about any graveyard in the area. Roman tomb found in a close proximity to the church has been found completely by case and in this sense finding graves without the use of GPR would be very difficult task.

1.4 THESIS OBJECTIVES

The objectives of the master thesis are as follows:

- to identify the precise location of known archeological feature (road);
- to search the area and identify the features for whose existence precise historical data were not found (oratorio, cemetery).

To achieve the objectives the following operations should be included:

- detailed field survey and data collection;
- data examining and processing using 2D and 3D module of REFLEX;
- examination and interpretation of the results, with the final aim of identifying the subsurface features.

2.GPR FRAMEWORK

2.1 HISTORY OF GPR APPLICATION

The first attempt in applying GPR was made in 1920s in Austria, to determine the thickness of the ice in the glacier. The aspects of the technology remained mainly forgotten until 1950s, when US Air Force radar on board technicians noticed that their radar pulses were penetrating the glacial ice flying over Greenland. A number of mishap occurred since airborne radar analysts were detecting the bedrock surface below the ice interpreting it as a ground surface, neglecting the ice above and almost causing planes to crash into glaciers. Realization that radar is able to penetrate ice led to various experiments with ice and other materials, such as soil and water. [7]

As a result, the first GPR prototype was designed in 1967 by NASA (National Aeronautical and Space Administration) and sent on a mission to the Moon to determine surface conditions prior to arrival of manned vehicle. In the 1970s it was recognized the ability of GPR to detect to locate buried objects, such as pipes, tunnels, mine shafts etc. At the same time geologist and hydrologists began to investigate buried and surface soil units.[7] The development has been continued in future, both in the field of the GPR devices design and processing techniques. The advancements in the field of portable computers (especially birth of the Epson HX20 portable microcomputer in the early 1980s) have strongly influenced the field. [9]

The existence of numerous lossy dielectric material environments combined with the broad radio frequency spectrum led to a wide range of GPR applications. It is often said that applications of GPR are limited only by the imagination of the people and availability of suitable instrumentation and processing techniques. Similar methodology can be applied to glaciology and to nondestructive testing of concrete structures; the spatial scale of applications varies from kilometers to centimeters. [10]

2.2 THE PHYSICS OF ELECTROMAGNETIC WAVES

GPR signals are electro-magnetic (EM) waves. The physics of EM waves is mathematically described by Maxwell's equations and together with a relationships which quantify material properties, forms the base for quantitative description of GPR signals. [10] Basically, Maxwell briefly summarized the work of numerous researchers in this compact form. From these relationships, all classic EMs (induction, radio waves, resistivity, circuit theory, etc.) can be derived when combined with forms to characterize material electrical properties. [4]

$$\bar{\nabla} * \bar{E} = -\frac{\partial \bar{B}}{\partial t} \quad (1)$$

$$\bar{\nabla} * \bar{H} = \bar{J} + \frac{\partial \bar{D}}{\partial t} \quad (2)$$

$$\bar{\nabla} * \bar{D} = q \quad (3)$$

$$\bar{\nabla} * \bar{B} = 0 \quad (4)$$

where: E is the electric field strength vector (V/m); q is the electric charge density (C/m³); B is the magnetic flux density vector (T); J is the electric current density vector (A/m²); D is the electric displacement vector (C/m²); t is time (s); and H is the magnetic field intensity (A/m).

Equation (1) represents Faraday Law which says that a time varying magnetic field cause charges to move, generating a closed loop electric field. Equation (2) represents Ampere Law, which states that electric currents generate magnetic field. Equation (3) states that electric charges are sources (or sinks) of electric field. Electric fields emanate from electric charges. Time varying electric fields will be of closed loop form when induction (Faraday's observation) occurs. The electric field will emanate outward (or into) when free charge is the field source. In general, both field characters will be present and superimposed for time varying signals. Free magnetic charges

have never been observed in nature; as a result, magnetic fields must form closed loops which explains Equation (4) and distinguishes magnetic flux behavior from electrical field character. [10]

Maxwell summarized the work of numerous researchers in this compact form. From these relationships, all classic EMs (induction, radio waves, resistivity, circuit theory, etc.) can be derived when combined with formalism to characterize material electrical properties. [4] Electro-magnetic (EM) waves are emitted in a cone (the 'cone of transmission'), which spreads out with increasing depth below the surface. The dimensions of the cone are determined by the encountered subsurface conditions and by the frequency of the energy being transmitted into the ground, with higher frequency energy resulting in narrower cones of transmission. [7]

The transmitted energy is not limited to the centre frequency of the antenna being used. GPR transmits energy in broad band, generally with a two octave bandwidth, meaning that a range of frequencies between one half and two times the centre frequency of the antenna will be emitted (for example, a typical 500 MHz transmitter produces frequencies from about 250-1000 MHz). [6]

Ground penetrating radar exploits the wave character of EM fields. Maxwell's equations describe a coupled set of electric and magnetic fields when the fields vary with time. Depending on the relative magnitude of energy loss (associated with conductivity) to energy storage (associated with permittivity and permeability), the fields may diffuse or propagate as waves. Ground penetrating radar is viable when conditions yield a wave-like response. Depending on the relative magnitude of energy loss (associated with conductivity) to energy storage (associated with permittivity and permeability), the fields may diffuse or propagate as waves. Ground penetrating radar is viable when conditions yield a wave-like response. [4]

At low frequencies, the electromagnetic fields diffuse into the material. The energy distributes itself in the same manner as heat. An impulsive signal gets smeared out (dispersed) because its frequency components are attenuated at different rates and travel at differing phase velocities. At high frequencies, the electromagnetic fields propagate as waves through the medium. All frequency components travel at the same velocity and suffer the same attenuation. An impulsive signal will travel with its shape intact. This is referred to propagation without dispersion. [10]

2.3 INTERACTION WITH THE SUBSURFACE MATERIALS

In the literature, to provide better understanding of mutual interaction of EM waves and subsurface materials, Maxwell's equations are usually accompanied by constitutive equations which describe material's response to EM waves. Electrical and magnetic properties of materials are of the great importance for GPR and these equations provide macroscopic (average) behavior of electrons, atoms and molecules when they are exposed to EM waves. [4]

$$\bar{J} = \tilde{\sigma} * \bar{E} \quad (5)$$

$$\bar{D} = \tilde{\epsilon} * \bar{E} \quad (6)$$

$$\bar{B} = \tilde{\mu} * \bar{H} \quad (7)$$

where: E is the electric field strength vector (V/m);

B is the magnetic flux density vector (T); J is the electric current

density vector (A/m²); D is the electric displacement vector (C/m²); σ is electrical conductivity

(mS/m); μ is magnetic permeability (N/A²) and ε is dielectric permittivity (F/m).

Electrical conductivity (σ) describes the ability of a material to conduct away the electric portion of the EM wave. Materials which are more electrically conductive will more readily conduct away the electric part of the EM wave, thereby dissipating or attenuating the wave and

resulting in shallow subsurface imaging; conversely, materials with a low electrical conductivity will allow greater depth of EM wave permeation. [6]

Magnetic Permeability (μ) describes the ability of a material to become magnetized in the presence of an EM field. Materials that are more magnetically permeable will more readily interfere with the magnetic part of the EM wave, thereby attenuating the wave and resulting in shallow subsurface imaging. Dielectric Permittivity (ϵ) describes the ability of a material to store and transmit an electric charge induced by an EM field. [6] The dielectric permittivity of a material is also described by its Relative Dielectric Permittivity (RDP or k), which is defined by the equation:

$$k = \frac{\epsilon}{\epsilon_0} \quad (8)$$

where: k is the RDP (-), ϵ is the dielectric permittivity of the material, and ϵ_0 is the permittivity of a vacuum (8.89×10^{-12} F/m).

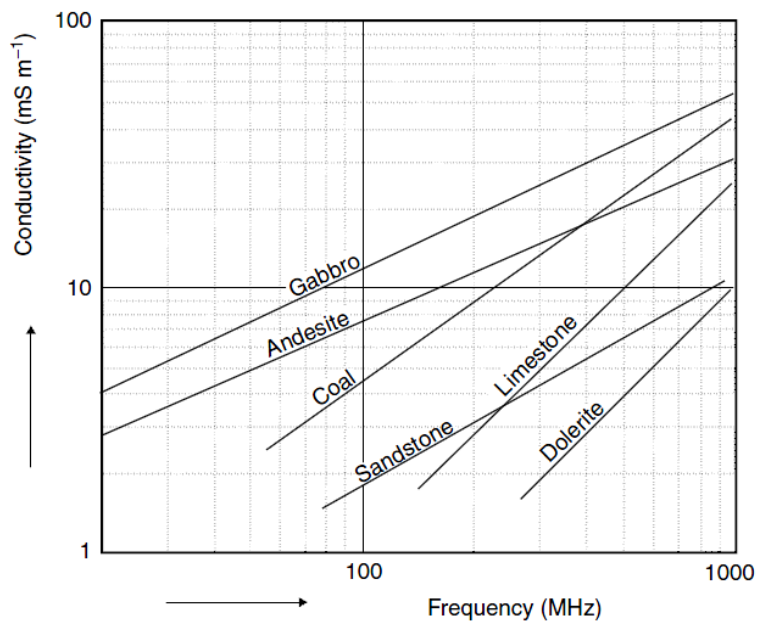


Figure (1): Approximate rates of change in conductivity with frequency at radar frequencies for some common rock types [11]

RDP can be used to estimate radar wave velocity and wavelength (or amplitude), with higher RDP materials having lower wave velocities and lower amplitudes. RDP can therefore be taken as a general measure of the depth to which radar waves will penetrate the ground. [6]

Material	Dielectric permittivity (ϵ) [-]	Electrical conductivity (σ) [mS/m]	Velocity (v) [m/ns]	Attenuation (α) [dB/m]
Air	1	0	0.30	0
Ice	3 - 4	0.1	0.16	0.01
Fresh water	80	0.05	0.033	0.1
Salt water	80	3000	0.01	1000
Dry sand	3 - 5	0.01	0.015	0.01
Wet sand	20 - 30	0.01 – 1	0.06	0.03 – 0.3
Shales and clays	5 – 20	1 – 1000	0.08	1 – 100
Silts	5 – 30	1 – 100	0.07	1 – 100
Limestone	4 – 8	0.5 – 2	0.12	0.4 – 1
Granite	4 – 6	0.01 - 1	0.13	0.01 – 1
Dry salt	5 - 6	0.01 - 1	0.13	0.01 - 1

Table (1): typical values for radar parameters for some common materials [11]

Ground penetrating radar is the most useful in low-electrical-loss materials, where energy dissipation is small compared to energy storage. If $\sigma = 0$, GPR would see very broad use since signals would penetrate to great depth. In practice, low-electrical-loss conditions are not prevalent. Clay-rich environments or areas of saline groundwater can create conditions where GPR signal

penetration is very limited. [4] While traveling down to the subsurface, different levels of interactions with subsurface materials are possible, mainly depending on the materials characteristics and incident angle of the waves. [6]

2.3.1 Reflection

When EM waves travelling through the subsurface encounter a buried discontinuity separating materials of a different physical and chemical properties, part of the wave is reflected off the boundary and back to the surface. These subsurface discontinuities may be the interfaces between archaeological features and the surrounding matrix, void spaces, or buried stratigraphic boundaries and discontinuities. The proportion and direction of the reflected EM wave are dependent upon the properties and shape of the deposit off which they are reflected. On a smooth, planar surface, the angle at which the wave will be reflected can be predicted based on the law of reflection, which states that the angle of incidence will equal the angle of reflection (with respect to the perpendicular and in the same plane). As the EM wave moves deeper beneath the surface, its signal weakens, and less is available for reflection. The strength of the reflected wave is also dependent upon the physical and chemical properties of the two materials from whose interface it is being reflected. [7]

2.3.2 Refraction

The part of the EM wave that is not reflected at subsurface discontinuities changes velocity, and in doing so is refracted or bent at the interface, resulting in a change in the direction of the wave through the ground. The angle at which the wave will be refracted can be predicted based on Snell's Law of Refraction: traction explains why the cone of transmission becomes increasingly narrow with depth. In addition, Snell's Law can provide the critical angle beyond which EM waves cannot propagate between two different materials. [7]

2.3.3 Diffraction

In physics, ‘diffraction’ refers to the bending of waves around objects, or the spreading of waves as they pass through narrow openings. Diffraction may occur around steeply sloping or vertical surfaces, resulting in increased radar wave travel time and therefore distortion of the depth, location, size, and geometry of the object. In the case where velocities change along the vertical axis of these objects, a phenomena known as pull-up and pull-down occurs; these terms describe the underestimation or overestimation of the depth of the lower boundary of the feature in question. In GPR theory, diffraction is more commonly applied to the phenomenon that produces point source hyperbolas. The hyperbolic image produced from point source reflectors is due to the fact that GPR energy is emitted in a cone, which radiates outwards with depth. As such, energy is reflected from objects that are not directly below the antenna; the reflection, however, is recorded as being directly below the antenna, and at a greater depth due to the oblique transmission of the wave. Only the apex of the hyperbola denotes the actual location of the point source. [7]

2.3.4 Scatter and focusing

The term ‘scatter’ is used to refer to the phenomenon of waves being reflected away from the range of the receiving antenna; such waves are not collected by the GPR. This phenomenon occurs on surfaces sloping away from the antenna, on convex up surfaces, in deep narrow concave features, and in near vertical features. Other generally resolvable features located near deposits that produce a high degree of scatter may also be obscured by this phenomenon. suggests collecting data in closely spaced perpendicular transects to reduce the effects of scatter. The opposite of scattering is focusing, which occurs when waves are reflected off surfaces sloping towards the antenna or within shallow wide concave up features. This results in high-amplitude waves being reflected back to the receiving antenna, and in some cases, multiple reflections within these features, which may distort depth, location, size, or geometry. [7]

2.3.5 Dispersion, dissipation and attenuation

As EM waves propagate to greater depths, they become increasingly dispersed due to the electrical conductivity of subsurface materials, until such point as they are fully dissipated or attenuated, and no energy is reflected back to the surface. The rate of attenuation or dissipation is relative to the frequency of the transmitted wave and the properties of the subsurface materials it encounters. Higher frequency waves are more readily attenuated, and therefore have shallower penetration depths. It is important to note that waves experience dispersion, dissipation, and attenuation in both vertical directions – reflected waves may be attenuated on the way back to the receiving antenna, and will therefore not be collected. [7]

2.3.6 Multiples, ringing, and reverberation

Multiples or ‘ring-down’ occur when EM waves encounter highly-reflective or impermeable objects (such as metals), and are due to multiple reflections between the metal object and the surface. The result is multiple stacked reflections being imaged below the metal object. Ringing refers to system noise produced from the antennas, and is visible in reflection profiles as horizontal banding, usually in the upper portion of the profile. Reverberation, like ring-down, produces multiples in reflection profiles, but it is a result of system noise produced from ‘ringing antennae’ which reverberate when spaced too closely. [7]

2.3.7 Background Noise and Clutter

Not all waveforms collected are due to subsurface reflections. Especially in the case of unshielded antenna, reflections may be collected from nearby above ground objects, such as buildings and trees; these generally produce high amplitude linear reflections. Background noise may also be generated by other nearby sources of EM waves, including televisions, cell phones, and radio transmission antennas; GPR survey can be especially compromised by background signals in

areas near airports, military bases, or busy roads. The GPR antennae also contribute to background noise, in a way that they produce an EM field that obscures signals within 1.5 wavelengths of the antenna. Background noise produced from subsurface reflections is termed clutter, and refers to point targets and small discontinuities that reflect energy and obscure the signals of other more important reflected waves. Clutter can be minimized if we select antennas of lower frequency, which will not detect small objects. [7]

2.3.8 Attenuation

It is important to note that attenuation always occurs when EM waves are emitted to the ground. It is a function of four general factors and each of them we should account for. The first one are *coupling losses*, which occur when the radar antennas are not placed in direct contact with the ground, or when the ground surface is uneven, allowing radar energy to be scattered and lost before it effectively “couples” with the ground. This loss factor can be mostly overcome by making sure that GPR instrumentation is moved slowly and carefully along the ground surface, with antenna attached to the ground. [7]

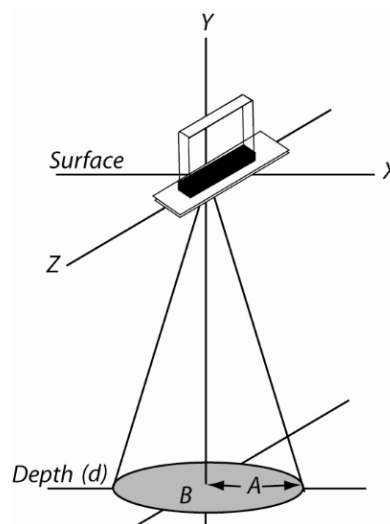


Figure (2): cone of transmission spreading down the subsurface.

Another factor is *geometric spreading* which occurs when energy is moving into the ground. This loss is a function of the conical shape of the transmitted radar pattern and the fact that the energy is spread out over a larger and larger surface area as it travels deeper in the ground. Spherical spreading with depth decreases the amount of energy that can be reflected back to the surface from any buried object or interface below, lowering the effective resolution of any reflections generated. This is a factor inherent in the method and cannot be adjusted for using standard GPR equipment. [7]

A third site-specific factor is *energy scattering*, which can be caused when radar energy reflects in random directions from buried objects or discontinuities in the ground, redirecting some of it away from the surface receiving antenna so they are not recorded. *Electro-magnetic attenuation* is a fourth and probably the most important site-specific factor in determining the GPR method's effectiveness. Radar energy is composed of both electrical and magnetic waves, which move in a conjoined fashion, the removal of either one or the other by electrically conductive or magnetically permeable ground effectively destroys the transmitted energy. In general, soils that are wet and have high clay content, especially clays of a certain mineralogy, will have high electrical conductivities as measured by their cation exchange capacity (CEC). In those clay soils, ions absorbed on some clay minerals could undergo exchange reactions with ions in the water, which increases the electrical conductivity of the ground. While most studies of GPR effectiveness evaluate clay as a general constituent, clay mineral types vary considerably with respect to their electrical properties. [2]

2.4 AMPLITUDE ANALYSIS

The most important precondition for detecting an object is that object re-emits some of the radio wave energy that falls on it. This requires that there should be a change in the electrical properties from the surrounding host material. As discussed previously, changes in dielectric

permittivity and electrical conductivity cause scattering of radio waves (electromagnetic energy). By detecting this scattered energy, it is possible to locate and position the sources of the scattered energy. [10]

The amplitude and speed of electromagnetic waves sent by the GPR unit increases or decreases as it passes through buried physical or chemical changes. As the waves encounter subsurface changes some of the energy is reflected back to the GPR unit and processed. The remaining energy continues through the ground until it attenuates and ceases propagation. This received energy creates a side-scrolling image of subsurface features and buried areas of higher and lower amplitude. This data is then interpreted by the operator to determine the locations, depths, and materials that caused the reflection.[5]

Certain buried targets create unique GPR reflections. An understanding of why each type of signature appears as it does will allow the researcher to interpret many common subsurface anomalies while in the field. This will in turn cut down on post acquisition processing time. Although there is some consistency in the identification of the major target types, there is rarely a way to identify exactly what material the target is made of. However, in respect to subsurface anomalies, the greater the amplitude of wave reflections through a medium, the greater the difference in physical and chemical characteristics of the buried material. The change in contrast on the GPR profile, either isolated regions of high or low contrast or amplitude may be analyzed to understand the possible material compositions of buried targets.[5]

2.4.1 Metals

The GPR signals cannot penetrate metal objects. This phenomenon creates high amplitude signals of repeating or “echoing” bands upon the screen, as shown in Figure (3). This results as the

electromagnetic wave bounces back and forth from the highly reflective metal object to the GPR device over and over again. Very small metal objects may not appear on GPR profiles, especially with the use of low frequency antennas. However, metals are often visible in shallow settings with high frequency antennas. The reflected signature from metals is at most times unmistakable. However, other dense or reflective buried items are capable of creating echoes, such as ceramics or concrete. The most commonly encountered metallic objects are rebar ring, metal piping, or covered metal scraps.[5]

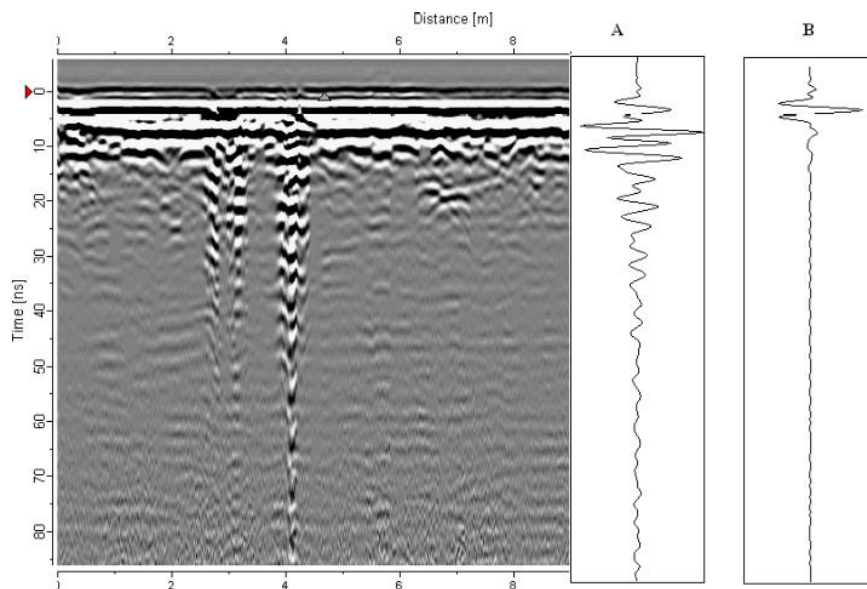


Figure (3): ringing effect created by a reflection from metal object.

2.4.2 Point-Source Reflections

Point-source reflections are displayed as parabolas on GPR profiles, as shown in Figure (4). The object that creates the point-source reflection is located at the apex of the arc. The attributes of the parabola may be analyzed in order to gain an understanding of the material composition based on the contrast, size, extent or reach of the arms, and curvature of the parabola. [5]

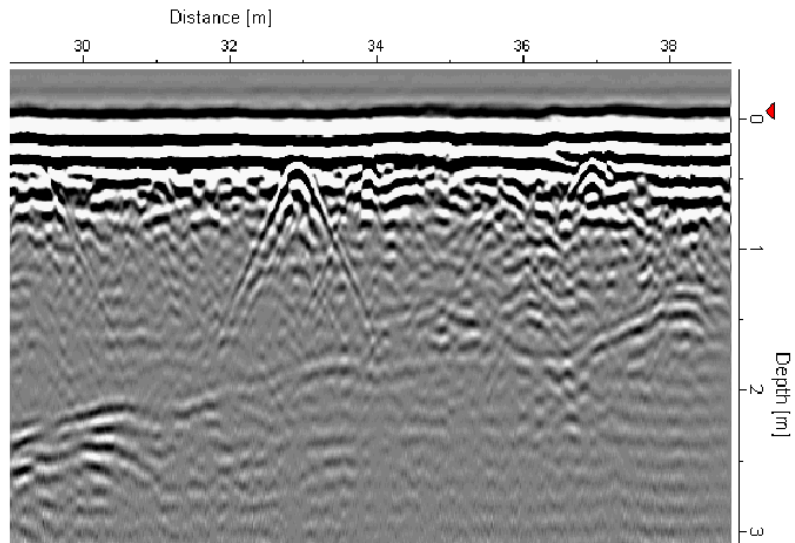


Figure (4): parabolic response of point source reflectors, typical for pipes.

2.4.3 Planar Reflections

Reflections from buried targets that do not appear as parabolas often take the form of planar reflections. These appear as horizontal anomalies, and contain alternating light and dark bands that exhibit higher amplitude in relation to the surrounding matrix.

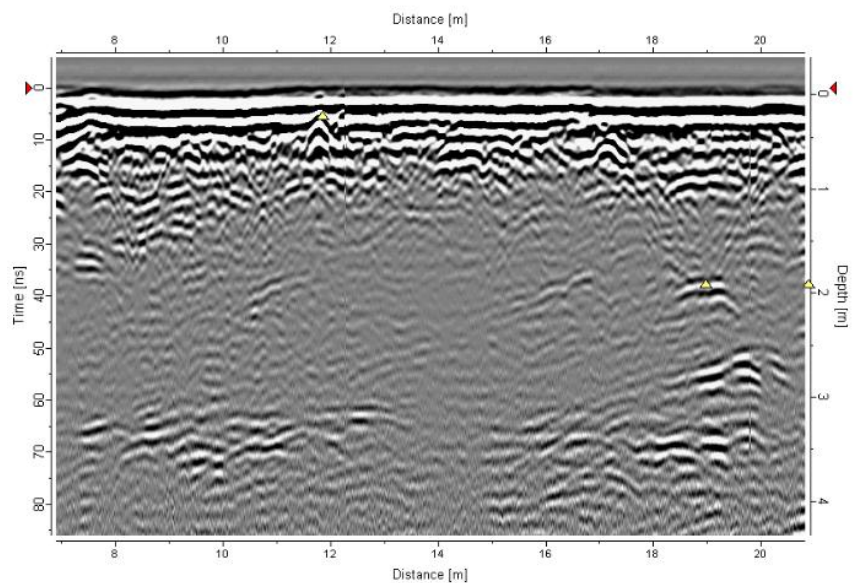


Figure (5): image showing the response planar reflectors, in the right part of the image (marked with yellow).

These reflections are often the result of a stratigraphic horizon, or a physical discontinuity such as the water table, or a horizontal feature of archeological interest. On the Figure (4) it is showed the presence of a planar reflection at the ancient coastal village of Aganoa, American Samoa. The upper layers are highly disturbed and contain multiple point-source reflections.[5]

2.5. DEPTH DETERMINATION

Determining the depth of a GPR survey can be accomplished by several methods:

- making laboratory measurements of the dielectric and conductivity;
- placement of a known object at depth to measure the two-way travel time;
- wide angle measurement using separated transmitter–receiver antenna;
- matching the shape of hyperbolas detected on the GPR radargram.

The first method involves collecting of samples of material at a site and then performing geophysical measurements back at the laboratory. One essential problem with performing laboratory measurements is that it is difficult not to disturb the material, and the in situ properties can be lost during extraction and transport. The second method of burying an object in the ground and then measuring the two-way travel time to the object provides reasonable estimates. However, usually the ground has been disturbed above the emplaced target and the measurement may be corrupted. Often a two-way travel time may be measured near a cut in the ground and an object can be inserted from the side so as not to disturb the upper material. This method provides a closer measurement to the microwave velocity at a site. [4]

In wide-angle measurements (sometimes referred to as “CMP”) the travel–time slope of a reflecting surface is used to provide an estimate of the microwave velocity. This method requires a flat reflector at depth and relatively homogenous materials over the length of the field measurement. [4]

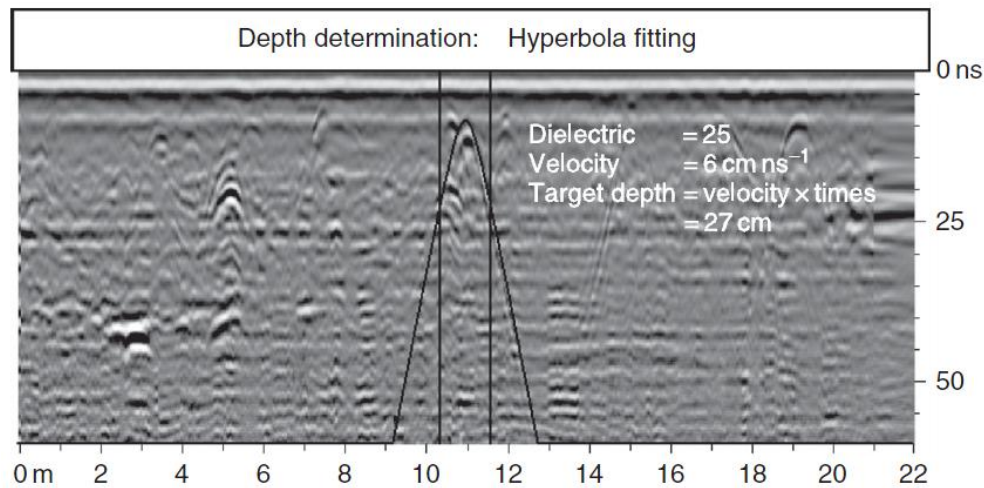


Figure (6): example of matching a hyperbola to raw field data; the shape of the hyperbola gives a measure of the microwave velocity of the ground. Narrow hyperbolas indicate slow microwave velocities in the ground; broad hyperbolas indicate higher velocities.

The fourth method involves matching of hyperbola observed on recorded radargrams and is the best method for remotely measuring the electrical properties of material. The width of hyperbolas recorded off small (point source) objects is the “DNA” of the ground which provides an estimate of the microwave velocity. The narrower the hyperbola, the slower the microwave velocity is; the wider the hyperbola, the faster the microwave velocity of the ground surrounding the target is. In the Figure (6) it is shown the matching of hyperbola seen in data collected at a Native American burial site in Louisiana. [4]

2.6 GPR IN ARCHEOLOGY

Archaeological geophysics has gained enormous popularity in the past decade within the archaeological community. For archaeological applications, radar antennas are moved along the ground in linear transects, creating two-dimensional profiles of a number of reflections and producing at the end a profile of buried features along each line. The most widely used frequencies are the one close to 400 MHz. They transmit energy up to about 3 meters in depth in many ground

settings and typically have a feature resolution of about 30 to 40 cm, which is usually considered perfect for archaeological identification. With the 400 MHz antennas transect spacing is usually 50 cm or less, which creates a footprint of energy transmission in the ground giving complete coverage of enclosed materials. By recording wave amplitudes from the two-dimensional parallel profiles it is suitable to create very accurate three-dimensional images of buried features. [2]

The two most important parameters for archeological acquisition are resolution of buried materials and depth of investigation. These two variables are inversely related and an analysis of them is vital when choosing the appropriate frequency antenna to use for data collection. Higher frequency antennas, above about 400 megahertz (MHz), are capable of better subsurface resolution, but fail to transmit energy to deep subsurface. Lower frequency antennas (in the 100–200 MHz range) can theoretically transmit energy that penetrates 5 m or more, but are incapable of resolving objects or interfaces smaller than about 60 cm in dimension. It is often argued in the literature that the depth of penetration is the most important factor in determining GPR effectiveness as some ground conditions. [2]

Beside resolution and depth of investigation which are related to frequency choice, GPR surveys are highly dependent on soil and sediment mineralogy, clay content, ground moisture, depth of burial of features, surface topography, and vegetation. For successful acquisition, one has to be aware of subsurface geological properties of the soil, otherwise it risks to misinterpret the results. Although by theory GPR use is not suitable and even not possible in soils saturated with water and clay, there are examples that have proved that even in such conditions it is possible to obtain relatively good results. This can be explained not by individual presence of clay or water, but with the difference in mineral composition of the clay and dissolved salts in the water that can cause higher or lower attenuation. [3]

Probably the most important feature of GPR highly exploited by archeologists is the fact that the subsurface archaeological features can be resolved in real depth. This is always very important in archaeological contexts because accurate depth is a vital element in planning future excavations, based on the results of a GPR survey. Prior to this, good velocity analysis has to be performed using a number of field collection and processing procedures. [3]

3. FUNDAMENTALS OF GPR DATA PROCESSING

GPR profiles often do not look like it is expected from archaeological features, so usually a great deal of experience is necessary for correct data processing and interpretation. A raw or processed GPR *trace* is recorded as a series of digital values equally spaced in time. It can be displayed either as a simple curve (*wiggle trace*), or by the *variable area* method in which excursions on one side of the zero line are shaded. Color is also sometimes used, either to shade excursions of one polarity in red and of the other in blue, or to shade an elongated rectangle according to signal amplitude and polarity. An ideal *variable area* trace would consist of a flat line punctuated by occasional ‘events’ produced by energy arriving at the surface after reflection from points vertically below the mid-point between receiver and transmitter aerials. A GPR *section* is created by plotting traces side by side, producing a record on which the horizontal axis represents distance and the vertical scale is in two-way reflection time. [11]

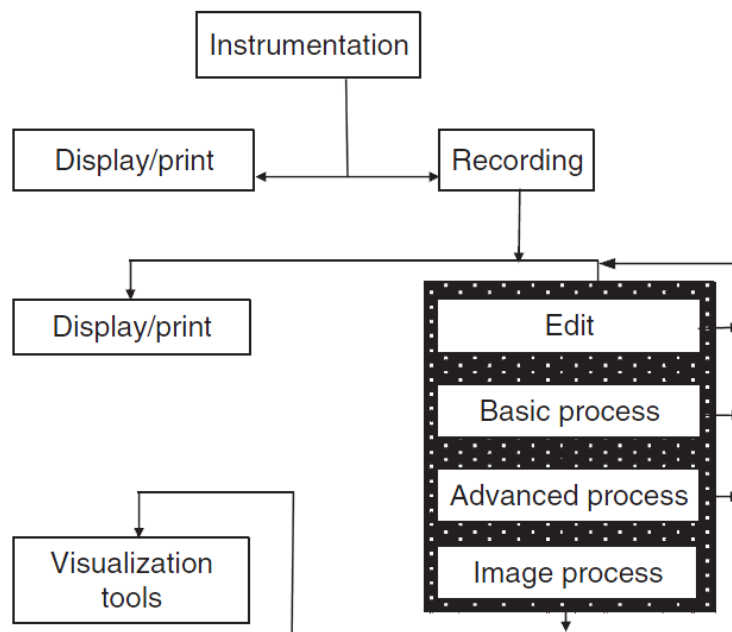


Figure (7): overview of a typical ground penetrating radar (GPR) data processing flow. Processing can vary from simple editing to total transformation of GPR information.

On the Figure (7) it is shown typical processing flow of GPR data, which starts with data acquisition and real time displaying or printing of raw data. The highlighted part on the right side of the image represents typical processing sequence. In many applications the real-time display is used for on-site interpretation and may be the end point for the radar survey. Normally data are recorded and available for post-acquisition processing and re-display. The areas of data processing have been grouped under the headings: data editing, basic processing, advanced processing, and visualization/interpretation. GPR data processing is usually an repetitive, iterative activity. A data set will flow through the processing loop several times with the data changes visually monitored by the processor. Straight through batch processing may be applied on large data sets after iterative testing on selected data samples. [10]

3.1 DATA EDITING

Once data are recorded, the first step in processing is data editing. Field acquisition is rarely so routine that no errors, omissions or data redundancy occur. Data editing encompasses issues such as data re-organization, data file merging, data header or background information updates, repositioning and inclusion of elevation information with the data. [10]

Data editing is often thought to be the simplest operation but different authors states that is usually most time consuming operation. It is very important since it has to ensure that further data processing is done without problems, and as such, it is essential before processing takes place. [10]

3.2 BASIC PROCESSING

One of the main requirements for methods used in basic processing is to leave the data sets reasonably intact. In other words, the processing should not radically distort the information from that which was collected. In general the degree of distortion is subjective and obviously excessive

bandpass (or any other) filtering can drastically alter a data set. Normally minor changes to the overall data set occur if simple basic processing steps are applied intelligently. [10]

3.2.1 Dewow

Due to the close proximity of receiver to transmitter the field near the transmitter contain low-frequency energy associated with signal saturation due to early wave arrivals, inductive coupling effects, and/or instrumentation dynamic range limitations. This low frequency energy often yields a slowly time-varying component to the measured field data and causes the base level of the received signal to bow up or down. This effect has become known as baseline “wow” in the GPR lexicon. [4] Dewow (or signal saturation correction) applies a running average filter to each trace to remove the initial DC signal component and low-frequency “wow,” which is highly recommended be applied to all data sets before any other processing steps are undertaken. [6]

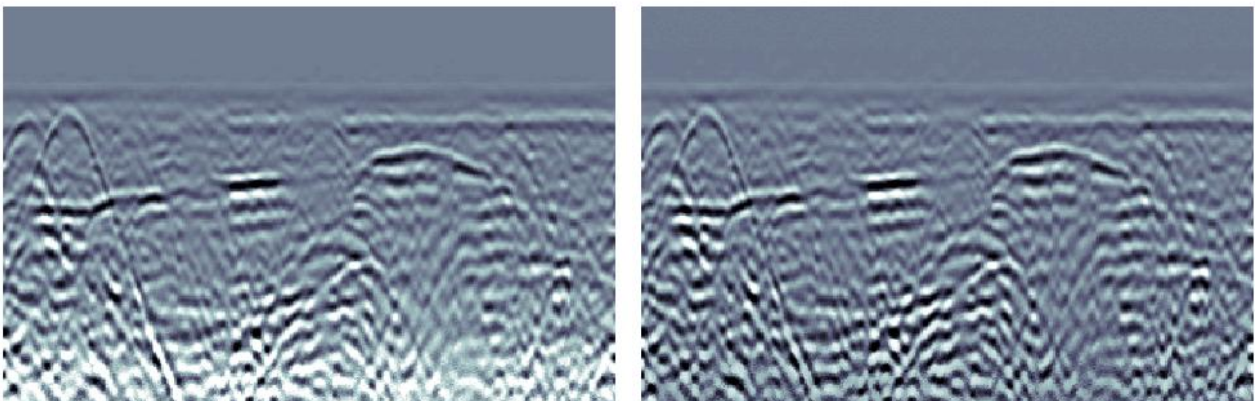


Figure (8): A profile before (left) and after application of dewow (right). Both profiles have gain applied.

3.2.2 Time gain

The next step of basic processing is usually to select a time gain for the data set. Radar signals are very rapidly attenuated as they propagate into the ground. Signals from great depth are very small and display of this information at the same time as signals from a shallower depths is difficult. [10]

Gains are used to boost signal strength, which generally decreases with depth, and enhance low-amplitude reflections. It is suggested in the literature to examine the average time-amplitude plots of the data before and after application of a gain to ensure the correct gain has been applied. Prior to application, the plot should show signal amplitude dropping, whereas after application of the ideal gain, signal amplitude should remain constant after its peak value. [6]

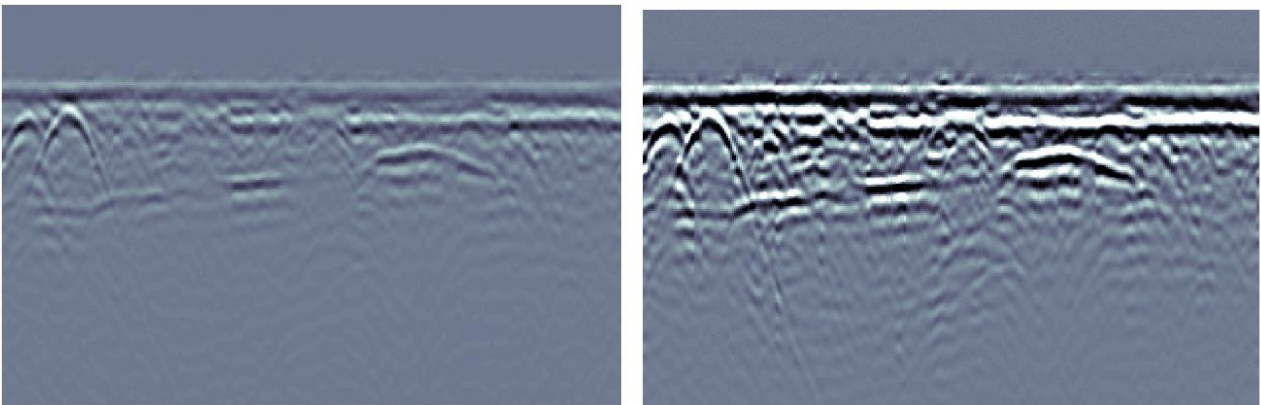


Figure (9): a profile after application of dynamic Automatic Gain Control – AGC. Profile has dewow applied.

Time gain has historically been very subjective and also very much display device dependent. Mainly two types of gain are applied, AGC (Automatic Gain Control) and SEC (Spreading & Exponential compensation) or energy decay. AGC applies a gain that is inversely proportional to the average signal strength, or the difference between the mean signal amplitude in a given time window and the maximum signal amplitude for the entire trace. It usually tends to over-gain the upper regions of reflection profiles, to the point that subtle features of importance may be easily obscured. On the other hand, if the gain applied is not of sufficient strength, the reflections at

the bottom of the profile are left relatively unaffected and without the required definition. If used carefully, however, AGC can usually provide excellent definition of local features within reflection profiles. [6]

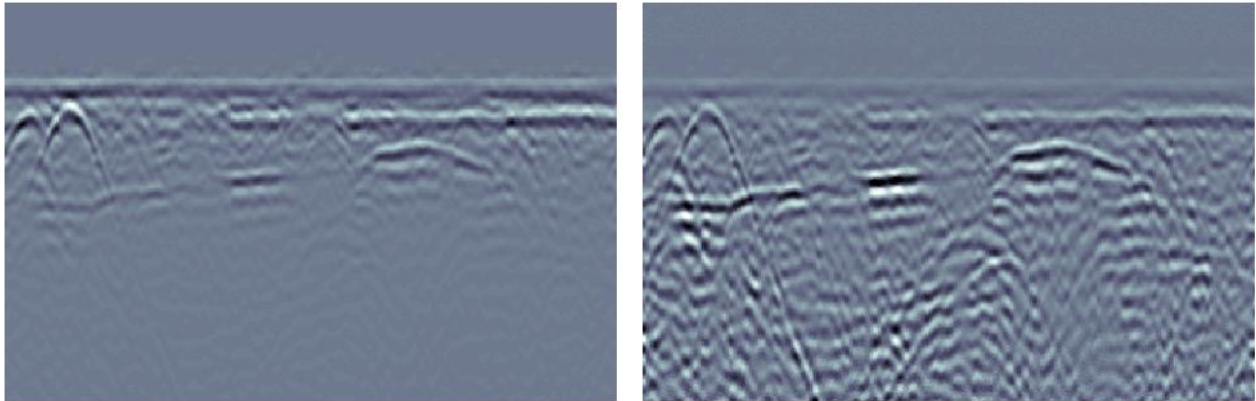


Figure (10): A profile before (left) and after application of manual SEC gain. Both profiles have dewow applied.

SEC gain applies an exponential gain that compensates spreading and attenuation of the propagating wave front. SEC tends to produce a more balanced reflection profile. The definition of more subtle features can be compromised, but there are other methods available to bring these features to the forefront [6]

3.2.3 Temporal and spatial filtering

This is often the next stage of the processing. Filtering can be applied before or after time gain as long as the effect of the gain is understood since time gain is a non-linear process. Temporal filtering means filtering along the time axis of the data set. A whole host of different types of temporal filtering may be applied from bandpass filtering using fast Fourier transforms (FFT) through to various types of linear and non-linear time domain convolution filter operators. In both cases the average amplitude spectrum for the whole section has been generated.[10] Spatial filtering

is performed in the horizontal (spatial) direction to enhance or eliminate certain frequencies and features. [6]

It is suggested by the literature to examine an average amplitude spectrum plot before and after applying a filter to aid in determining filter parameters. Prior to the application, the plot should show an irregular curve representing the frequencies present in the signal. Examining the plot again after application of a filter will show which frequencies have been removed from the spectrum. Usual filters used during basic processing are bandpass, lowpass, highpass, vertical and median. [6]

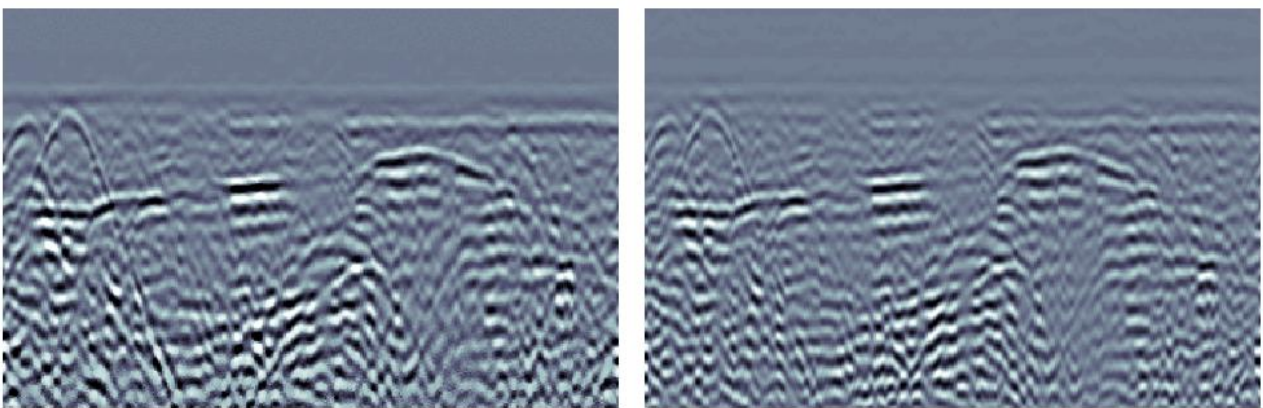


Figure (11): a profile before (left) and after application of a bandpass filter Both profiles have gain and dewow applied.

Highpass filtering of the A-scan data is a useful means of improving the signal to clutter ratio in situations where clutter is caused by additional low frequency energy generated by antenna ground interactions. In addition, excessive high frequency noise can usefully be reduced by lowpass filtering. [10]

Bandpass filtering is used to isolate a limited portion of the spectrum using Fourier transform, thereby removing high and low frequency noise and solving the problems. In this way both high- and low-frequency noise is removed simultaneously without significant influence on the bulk of the data. Due to this, it is at this level is usually enough to apply bandpass filter and the application of the other filters is not necessary. Also, it is also useful for isolating a specific range of frequencies for closer analysis. [6]

3.3 ADVANCED DATA PROCESSING

Advanced data processing addresses the types of processing which require a certain amount of operator bias to be applied and which will result in data which are significantly different from the raw information which were input to the processing. Such processes include well-known seismic processing operations such as trace attribute analysis, FK filtering, selective muting, normal move out correction, dip filtering, deconvolution, and velocity semblance analysis as well as more GPR specific operations such as background removal, multiple frequency antenna mixing and polarization mixing. [10]

3.3.1 Background Subtraction

Also known as average subtraction applies a running-average background subtraction to the data, subtracting the mean trace of a specific number of traces from each trace in the defined window, with the purpose of removing horizontal banding in profiles (due to system noise, electromagnetic interference, and surface reflections), thereby enhancing dipping events and obliterating horizontal events.[10] Average trace removal is a form of spatial filtering and it is one of the most common operations specifically applied to GPR data. [6]

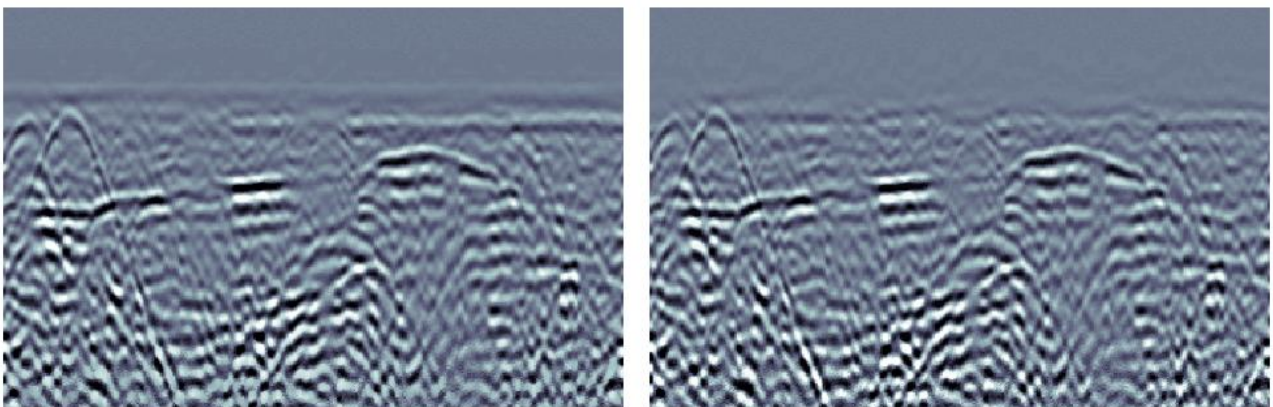


Figure (12): a profile before (left) and after application of background subtraction. Both profiles have gain and dewow applied.

Although being one of typical GPR data processing techniques, a number of authors recommend careful use of background subtraction in areas where there are suspected horizontal events of interest, and suggests highpass and lowpass filters as alternative options to remove horizontal banding. [7] It is widely used and mainly always part of GPR data processing, as it helps to remove banding in the upper regions of reflection profiles. In order to ensure that this filter will have little effect on the bulk of the data, the maximal number of traces allowable in the running average window. [6]

3.3.2 Deconvolution

It is an inverse temporal filter that compresses the recorded wavelets, thereby improving data resolution. The main purpose of deconvolution is normally to maximize bandwidth and reduce pulse dispersion to ultimately maximize resolution.[7]

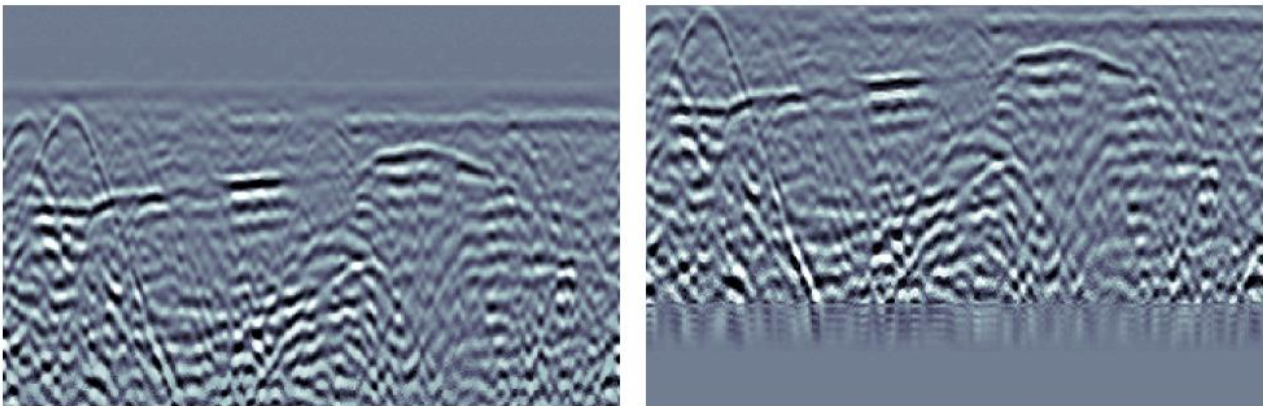


Figure (13): a profile before (left) and after deconvolution applied. Note both profiles have gain and dewow applied.

It can be used to remove multiples (repetitive horizontal reflections spaced at equal intervals) formed by multiple reflections between the surface and subsurface objects or layers, and convert radar wavelets to spikes. The deconvolution algorithm relies on the assumptions that

subsurface layering is horizontal with uniform intra-layer velocities, and that reflected waveforms have regular signals that do not scatter energy. [4]

By many authors has been noted however that much of this processing technique remains obscure and that it rarely has achieved great deal of benefit. [7] Part of the reason for this is that the normal GPR pulse is the shortest and the most compressed that can be achieved for the given bandwidth and signal-to-noise conditions. Instances where deconvolution has proven beneficial when extraneous reverberation or system reverberation is present. [4] Most of the practitioners recommend against its use.

3.3.3 Migration

It applies a synthetic aperture image reconstruction process to focus scattered signals, collapse hyperbolas to their apices, and reposition dipping reflections. Migration requires an accurate radar velocity and knowledge of the origin of the distorted reflections and wave travel paths before it can be applied to the data. It operates on a number of assumptions, including constant laterally invariant velocity layers; spatially uniform and spherically propagating source; no antenna separation; and no dispersion or attenuation. [6]

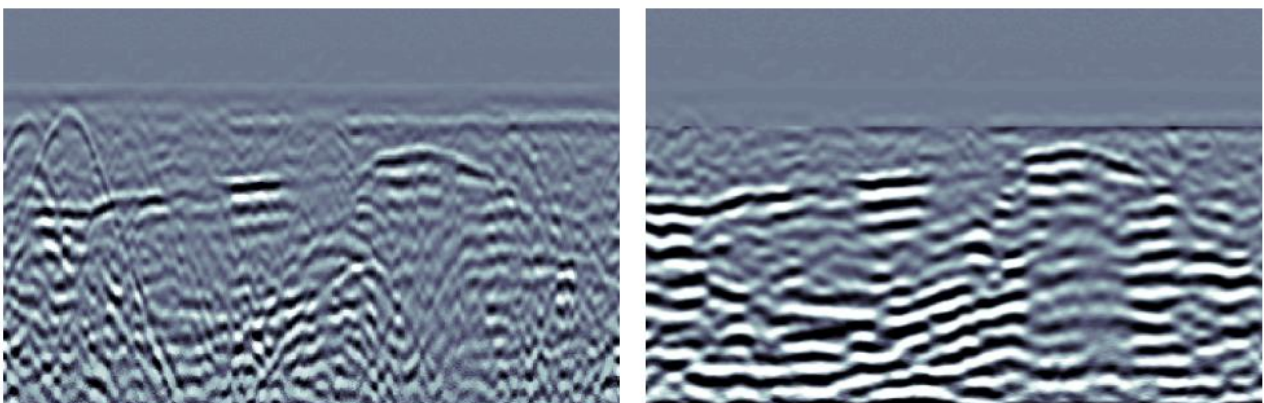


Figure (14): a profile before (left) and after migration. Note both profiles have gain and dewow applied.

A number of authors warns that migration may introduce false reflectors, and that it may distort reflections incorrectly.[7] One benefit to migration is increased image resolution. It is suggested that it is only when migration is applied that exact structural dimensions can be determined. [6] It is recommended to analyze data prior to migration, as the presence of hyperbolas may aid in detecting important subsurface features. [7] Correct velocity can be determined with the help of migration, as it is only at the correct velocity when inverse of the hyperbola appear. [6] The conclusion could be made that migration might be dangerous in the hands of a novice but powerful in the hands of a processor who has acquired the ability to use it effectively and recognizes the limitations. Migration is often an iterative process as background velocity is adjusted to optimize the migrated result. [10]

3.3.4 Attributes

Attribute analysis uses imaginary components of the data (calculated using Hilbert transform) to inform on relative or instantaneous reflectivity, amplitude, frequency, and phase relationships expressed in the data. These attributes are applied to the data in a moving time-space window to generate an attribute-based GPR section with true spatial distribution. Mostly three methods provides three options for attribute analysis: envelope, instantaneous phase, and instantaneous frequency [6]

Envelope (instantaneous amplitude) calculates the absolute value of each wavelet by converting negative wavelets to positive wavelets, resulting in a positive mono pulse wavelet. This process is used to emphasize the true resolution of the data, and can be used to simplify data and evaluate the signal strength and reflectivity. [6]

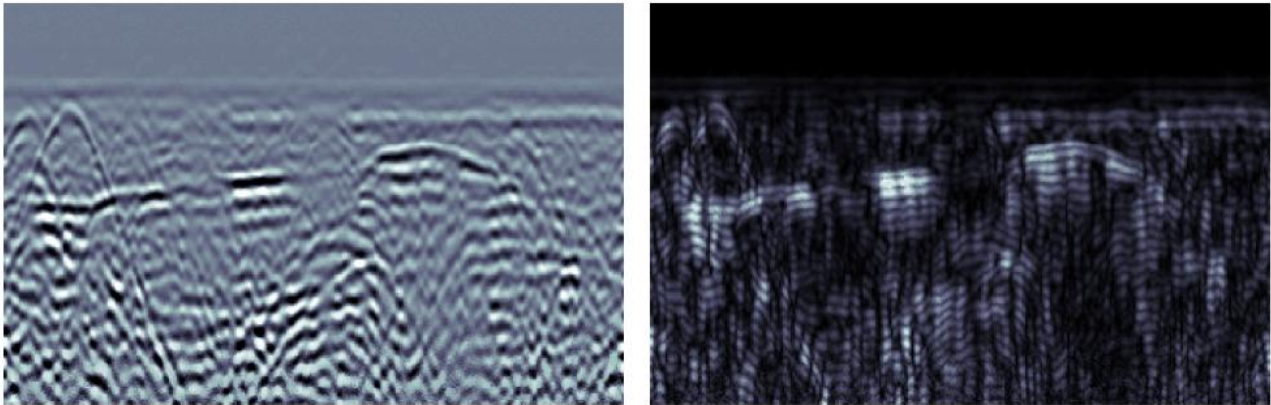


Figure (15): A profile before (left) and after application of envelope. Both profiles have gain and dewow applied.

The benefit of the envelope display is that it reflects the resolution of the data. One tends to get a false sense of resolution because of the oscillatory nature of the radar pulse. In fact the bandwidth or envelope of the pulse is what determines resolution not the time between zero crossings (which reflects the dominate frequency in the data). For this reason the envelope is extremely useful for generating more simple presentations which are representative of the data spatial resolution. that particular frequency will occur. Instantaneous frequency gives a rough feel for the texture on spatial scale of the GPR signal scattering sources. [10] Some authors warns against the use of attribute analysis in heterogeneous environments, as it can produce erroneous and inconclusive results. [6]

3.4 DATA VISUALIZATON

Initially, GPR data were always displayed as reflection cross sections (essentially vertical slices through the ground along the transect surveyed). As processing and computer processing power have advanced, more and more data presentation is in the form of 3D volume (voxel) rendering and time/depth slices (plan maps). The best results are obtained when migration and some

form of signal rectification or trace Hilbert transform envelope is applied. Today, 3D presentations are common as computer power and visualization tools have advanced rapidly. [4]

3.4.1 Volume visualization

Affordable access to 3D visualization tools and the rapid advance in computer technology are opening these tools to everyday GPR analysis. The degree of preprocessing needed to make these displays effective varies and encompasses all of the topics discussed here and more. The power of collecting reflection survey data in a tight grid and dumping it into 3D display software is enormous. Trends and subtle hard to correlate events become very visible when displays are animated. In general, these displays lose their impact when printed in hard copy form. [10]

4. GPR APPLICATIONS TO BURIED ARCHEOLOGICAL FEATURES - CASE STUDIES

4.1 A GPR SURVEY FOR ARCHEOLOGICAL INVESTIGATIONS IN AN URBAN AREA, LECCE, ITALY

GPR survey has been conducted in the urban part of Lecce using a 500 MHz antenna, with the main aim of exploring superficial layers and detecting potentially buried archaeological structures, identifying zones for excavations. Investigation was carried out mainly to prevent potential architectural remains from destruction, since a cultural center with an underground garage has been planned on site. Roman and Franciscan features were expected to be found in the area, due to the presence of an old Franciscan construction called “Caserma”, pulled down in 1971. The low penetration depth of the signal was due to presence of wet calcarenite (called by locals “Pietra Leccese”) and it was not exceeding 1 m and even using a 100 MHz antenna. The information was obtained only between the ground level and the top of the calcarenitic basement. [19]

Data were first recorded along parallel profiles, 1 m spaced, and the clear identification of the walls of the historical building was difficult because of the weak contrast in the electromagnetic parameters with respect to the hosting material (they were also constructed in “Pietra Leccese”). The spacing between sections was larger than minimal required for effective 3D processing, it was chosen due to lack of time and available space. On the other hand, the analysis of the radar sections allowed for identification and reconstruction of the shape and extension of a barrel-vault cavity, subsequently confirmed by archaeological excavations. Time slice representations were used as a tool to locate other features including modern-day urban utilities and the planimetric development of the barrel-vault cavity. [19]

The instrumentation used was Subsurface Interface Radar System 2 (SIR 2), manufactured by Geophysical Survey Systems (GSSI). It was equipped with two antennas with centre frequencies of 100 MHz and 500 MHz. Most of our work was used 500 MHz antenna, because the

resolution obtained with the 100 MHz antenna was too low to be effective for most archaeological targets of interest. [19]

A minimal processing was realized before analyzing the radar sections. The raw data generally show, as expected, low amplitude signals locally broken by very shallow reflections and for hyperbolically shaped anomalies characterized by high amplitudes. The quality of the original data did not require advanced processing techniques; in fact the application of different filters did not significantly improve the data quality. To recover, at least partially, the true shape of subsurface reflectors, a 2D migration routine was made. This technique, collapsing the diffraction hyperbolas due to small-scale heterogeneities, enhances the most significant events.[19]

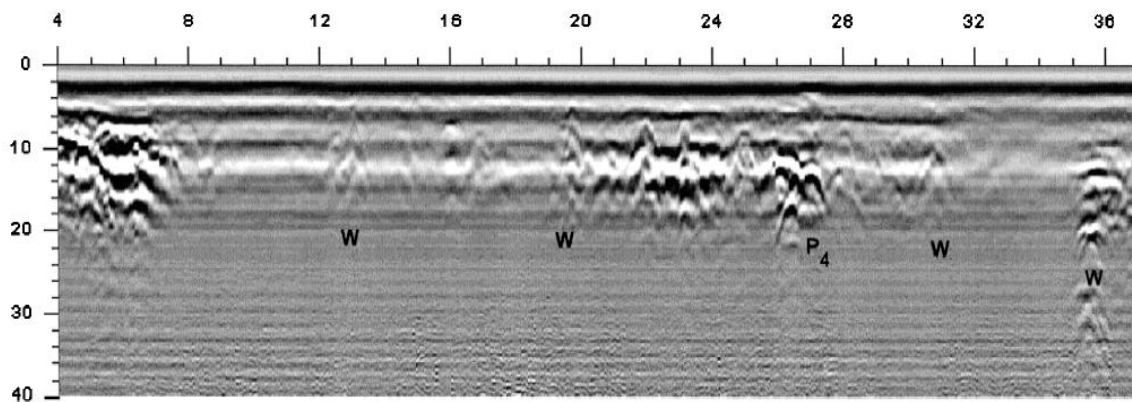


Figure (16): horizontal normalized radar section 500 MHz antenna. Note the attenuation zones between 7 and 20 m and between 27 and 35 m. Generally weak anomalies marked as W were found in correspondence of ancient walls, while P4 is a hyperbolic anomaly associated to a buried pipe.

Many anomalies (labeled with W in Figures (16) and (17)), although not easily recognizable in the sections, were found in quite close correspondence with the presumed position of the “Caserma” walls. Moreover, a great number of anomalies was also found outside the area presumably occupied by the building. Ground evidence and the analysis of the shape and alignment of the anomalies suggested that some of them (labeled with P) were related to the presence of public utilities. These anomalies are clearly visible in Figure (17).

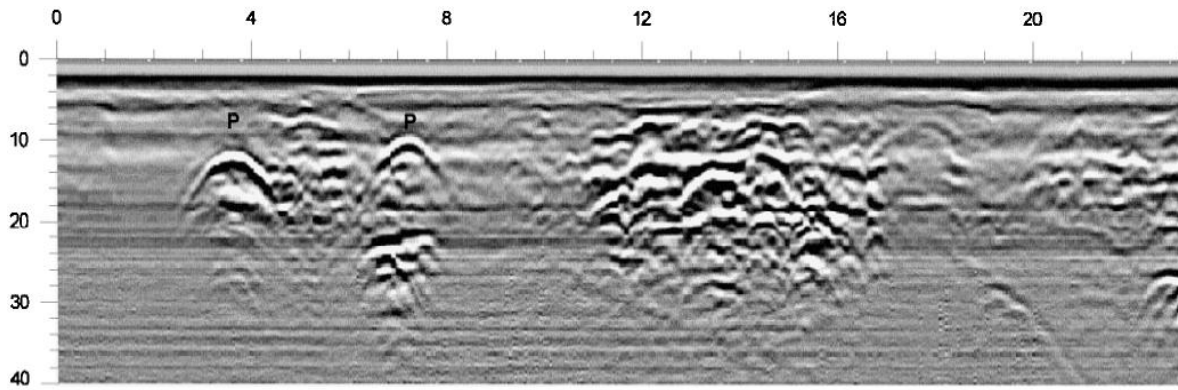


Figure (17): horizontal normalized radar section done with 500 MHz antenna. Pipe anomalies P and a chaotic reflection zone between 11 and 17 m. located near the southern boundary of the “Caserma” are evident.

The most interesting anomalies were found along both sets of orthogonal profiles shown in Figure (16). On the radar sections, they appeared as half-hyperbola or asymmetric hyperbola C in Figure (18) of almost the same horizontal extent (4–5 m) in both directions, between 22 and 30 ns. They are overlaid by strong near-horizontal reflections R in Figure (18) partially interfering with narrower hyperbolas. Comparing the different shapes of the curved anomaly C in the radar sections, it was argued that the structure responsible for that anomaly had a cylindrical top with axis oriented in an oblique direction with respect to the profiles. [19]

Excavation results confirmed the hypothesis made on the basis of the radar data. Excavation brought to light part of a SW–NE oriented barrel vault depth of the apex 0.65 m from ground surface, made of squared calcarenitic blocks standing directly on the calcarenitic basement, whose average depth in the excavation is 0.90 m. Boulders of sizes near the signal wavelength of the radar wavelength in ground 0.12 m are responsible for the diffraction hyperbolas observed on the radar sections. Through a small opening, under the top of the vault, it was seen that the cavity is now almost entirely filled with irregular stones and debris. [19]

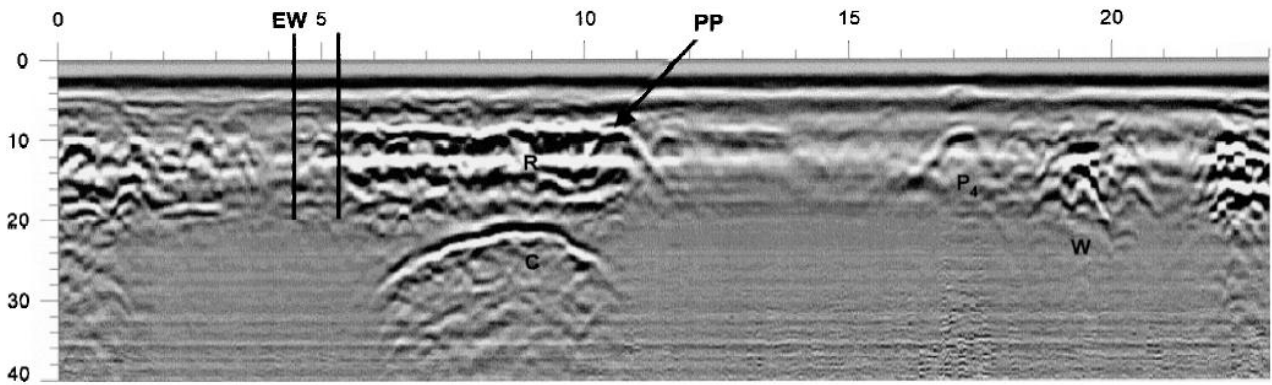


Figure (18): horizontal normalized radar section done with 500 MHz antenna. P4 and W indicate a pipe and a wall anomaly, respectively; C the curved anomaly associated to the barrel vault of an underground stone-filled cavity and R near-horizontal reflections due to different layers of reworked sediments. EW and PP are in correspondence to a stone wall and a couple of iron pipes revealed by the excavation.

Other archaeological features, uncovered during excavation, did not reveal such evident anomalies on radar sections. From Figure (18) a feature marked as EW was a stone-wall (width: 0.60 m, thickness: 0.60 m, depth of the top: 0.30 m, distance from the barrel vault: 1 m) in the radar sections shown in, made by regular “Pietra Leccese” blocks (0.60 x 0.25 m). It corresponds to zones characterized by weaker signals than the adjacent zones in radar sections and therefore was not identified in the preliminary analysis. This was because the weak anomaly associated with it is confused with the strong continuous reflections generated by the material in which it is immersed. Unlike the most frequent cases of stone-wall anomalies in literature, where the hosting material is characterized by weaker signals than that propagated in the wall. In this case there was opposite situation in which it was extremely difficult, if not impossible, to identify the relative anomaly. The features marked with P were a couple of iron pipes, of diameter 0.03 m, at depth of 0.40 m from the ground level. The anomaly associated with the pipes corresponds to the clearest hyperbola PP.

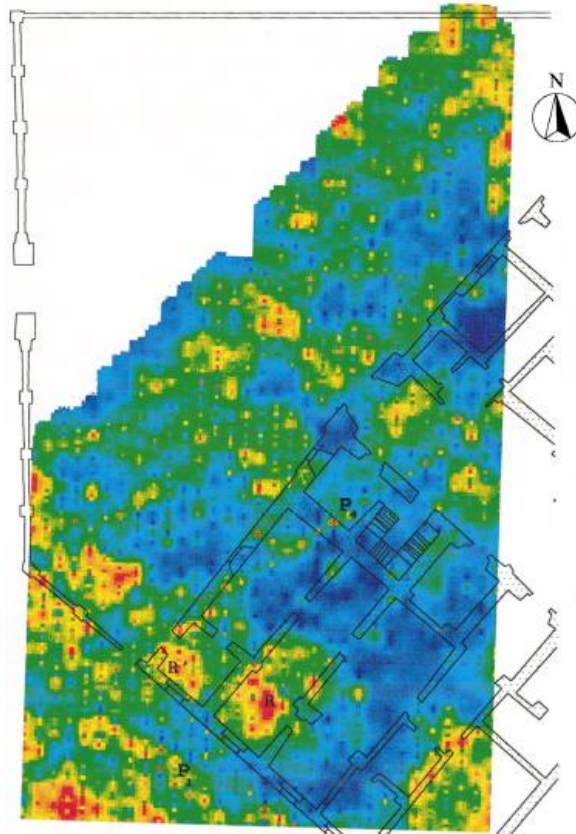


Figure (19): the most interesting slice 9 – 14 ns corresponding to 0.30 m below ground surface.

4.2 APPLICATION OF GPR IN DETECTING ARCHEOLOGICAL REMAINS IN BUYUK MENDERES GRABEN, TURKEY

This main topic of the study is the application of the Ground Penetrating Radar (GPR) to buried tectonic and archaeological structures in the Büyük Menderes Graben. The Büyük Menderes graben is rich in archaeological sites and there are ancient man – made structures, such as road, wall and bridge along the graben. It is likely that these man – made structures are offset by the fault or collapsed as a result of strong ground shaking. GPR studies were performed in 6 different locations along the graben, two of them are trench locations, three of them are offset archaeological features and one of them is buried archaeological feature. Both the 250 MHz and 500 MHz shielded antennas were used. [15]

Mapping of both the Roman Road and active faults showed that they intersect about 2 km west of Sultanhisar. The Roman Road climbs up a 7 m-high morphological scarp in east of Çakırçek stream. This morphological scarp is interpreted as the location of active fault. The base of the Roman Road includes marble blocks. Thus, it would be possible to identify marble blocks on GPR sections. GPR studies applied in this site to see the effects of faulting on the road and to locate the fault precisely. [15]

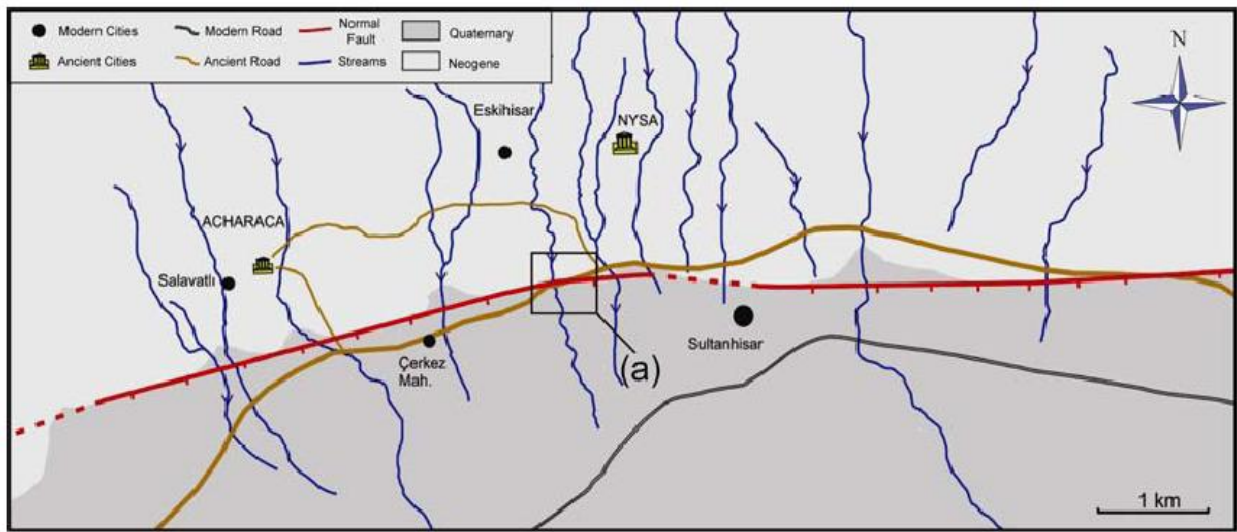


Figure (20) : Position of the Roman road and the fault zone near Sultanhisar. Probably, fault zone and the ancient road intersect at two locations in the west of Sultanhisar.

After data acquisition, basic processing steps have been applied. From the processed 250 MHz profile shown on Figure (21) the anomalous part of the profile is divided into two sub-sections shown on Figures (22) and (23). The processed and interpreted profiles of part 1 and part 2 are given in Figure (22) and Figure (23), respectively. The high contrast reflectors exist near the eastern and western sides of the profile but they disappear between 10 and 26 meters (Figure (21)). Detail sections (part1 and part 2) show that there are several short high contrast reflectors at different depths between 10 and 26 meters. [15]

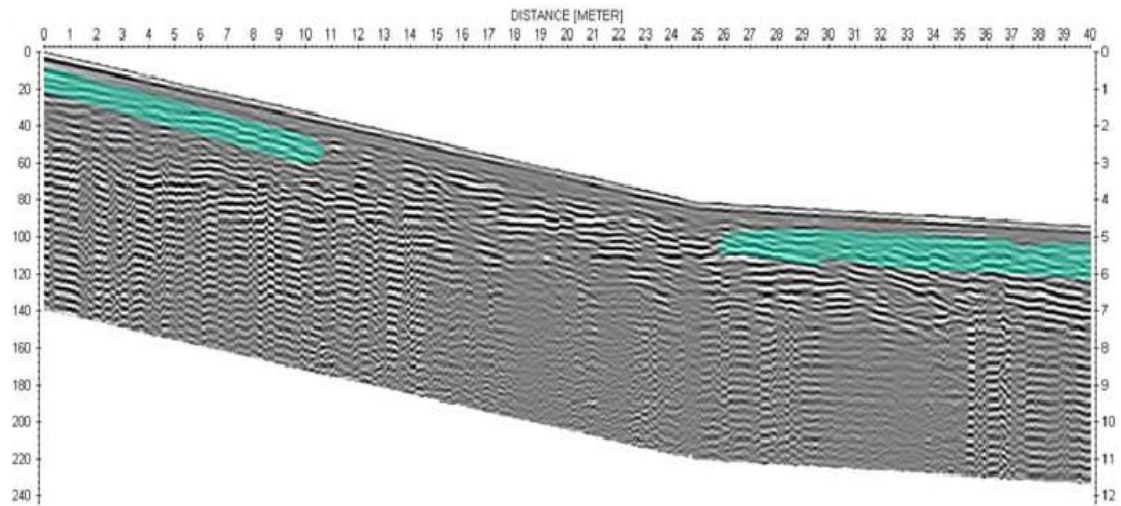


Figure (21): 250 MHz antenna profile of Roman Road. Processed data of GPR profile (blue highlighted areas represent high contrast reflectors).

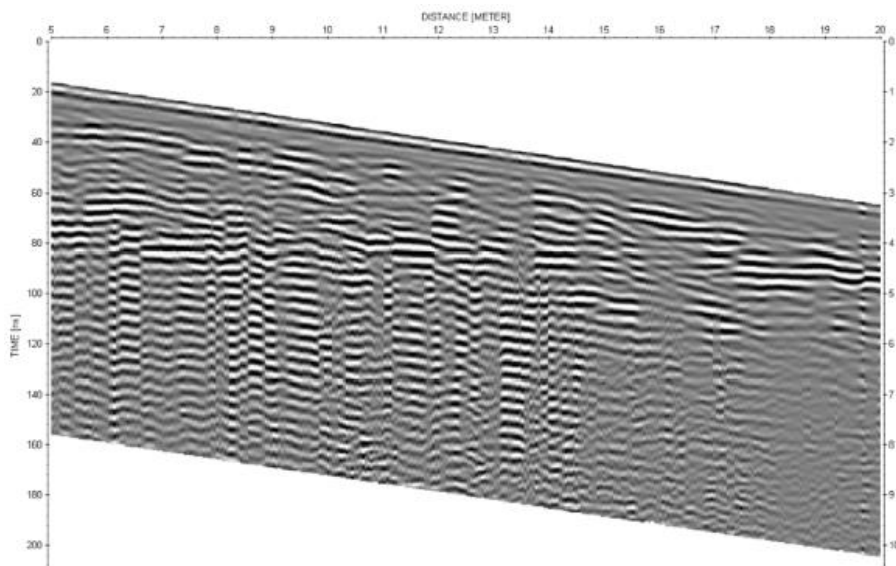


Figure (22): zoom view of the left part in Figure (21).

Detail sections (left and right part) are also showed that there are normal reflectors below the high contrast reflectors but they are offset in three locations by about 40, 50 and 90 cm (Figure (22) and (23)).

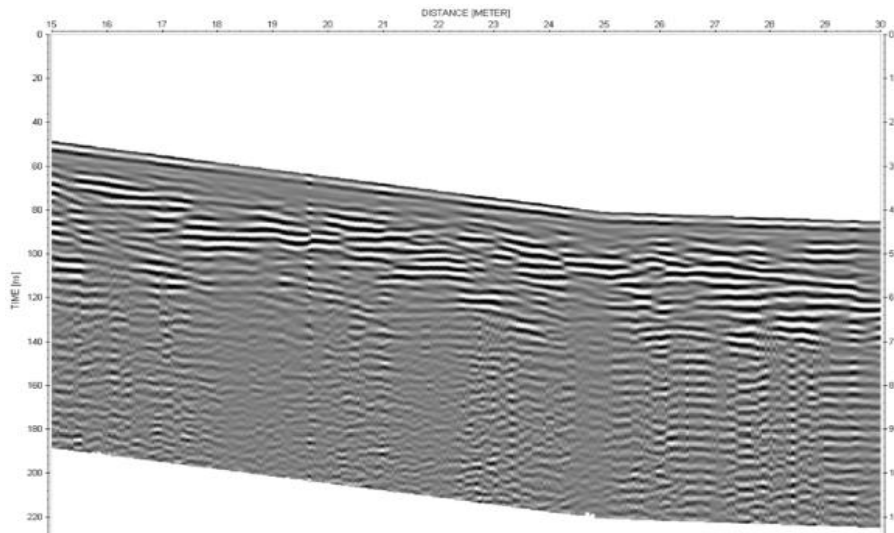


Figure (23): zoom view of the left part in Figure (21).

The same road was also measured with the 500 MHz antenna with the same processing steps. However, processed profile is not satisfying to make any interpretation because noise effect of the rough surface is high. Thus, interpretation of this location is based on only 250 MHz antenna. The high contrast reflectors probably represent the base of the Roman Road. Existence of high contrast reflectors at various depths between 10 and 26 meters suggests that the road was damaged. Occurrence of offset reflectors in three locations may suggest that this is a 16-m-wide deformation zone. GPR traces between 10 and 26 meters are noticeably flat than other traces out of this zone. This difference probably suggests that the damaged part of the road was filled (or repaired) by different material. [15]

5. SITE DESCRIPTION AND HISTORY

Brenna is located in Lombardy, 13 kilometers from Como, and today has almost 2000 inhabitants. Saint Adriano church is located in Olgelasca, part of Brenna, and that area has long religious pre-history, dating from pre-Christian era. The church itself had been constructed mostly in Roman era, who again had built the church on a Celtic ancient remains. During the Christian period, the area has been under strong influence of female monastery of Saint Vittoria di Meda, whose monks were very dedicated to the church. Today the church is located on the agricultural land outside of the village, on the edge of a forest. [16]



Figure (24): location of Saint Adriano church in Olgelasca, Brenna.

Romans arrived in Brenna – Olgelasca area in 196 ac. and the first colonies have been established soon after. Territory of Brenna has been divided in *centurie*, which are pieces of land of about 50 000 m², which were divided in such a way that every colonist was getting 1000 m². *Centurie* were given to the retired soldiers who have finished their military service. [16]

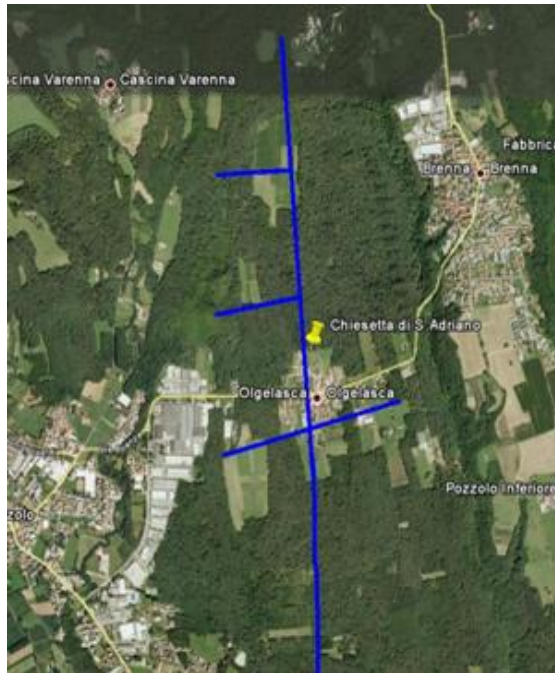


Figure (25): division of the area in centurie, blue line indicates the roads which were representing the border at the same time.

Today the evidences of Roman presence in area are few. One Roman tomb was found in the area in 1960 during excavation works, and 4 vases and one sword has been found. The tomb was used for cremation and it was constructed in the period between first and second century ac. [18]



Figure (26): archeological features found in Roman tomb discovered in 1960 Olgelasca, showing four remains of vases and one sword.

Another remains from Roman period is altar (Figure (27)) in a modest size (62 x 48 x 29 cm), which serves as a base for a rough stone column with a diameter of about 20 cm high and almost 2.60 m, topped by an iron cross. The monument has corroded and the inscription that was carved was destroyed in large part due to the niche dug out and closed with an iron frame in which the devotees were putting candles. [18]



Figure (27): the Roman altar found in Olgelasca.

The church is located on a relatively high terrain, approximately 80 cm above the surrounding land. As said before, this area has been long considered as sacred and there was no construction of any objects in close proximity of the church. The only man-made structure which is known to exist on the site is visible from the cadastral map dating from 1722. It was believed to be an ancient Roman road, extending in the direction north – south (in the Figure (28) it is directed horizontally). It was found in the literature that after the road has lost its significance, the local people have mainly taken the covering stone blocks, so it is belied that the road could be heavily damaged. Today, on site, it is not possible to see any remains of the road. [18]

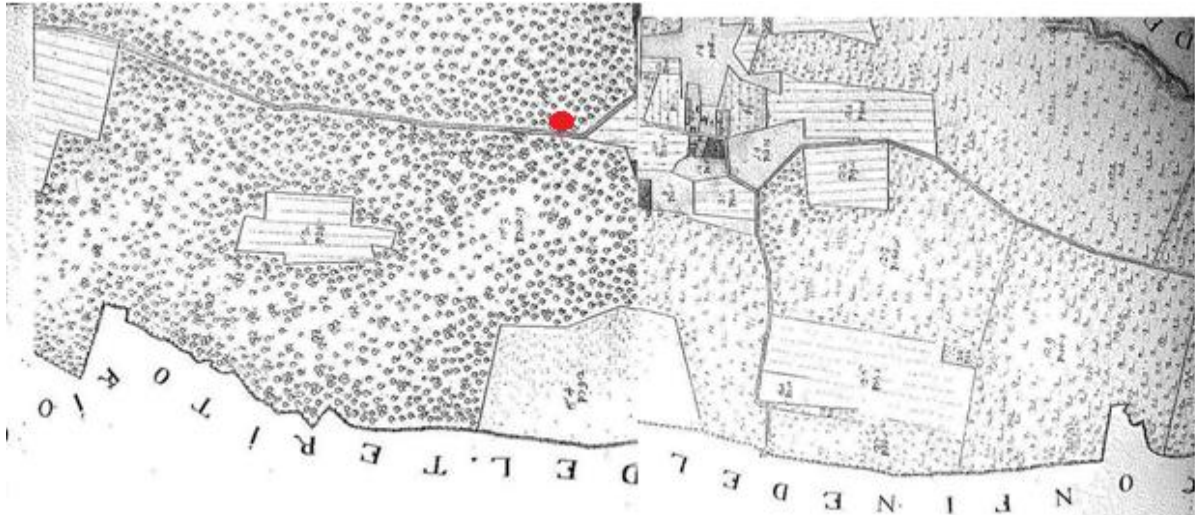


Figure (28): cadastral map of the area from 1722. The church is marked with red circle.

From the map it is possible to see that the church used to be in the forest, while today it is located some meters from the forest. There was also an argument between two groups of historians: one was claiming that an ancient oratorio used to be next to the church while the other was strongly against the idea. Also, there are no existing remains around the church which could indicate about the presence of oratorio.

6. GPR INVESTIGATION

6.1 INSTRUMENTATION

The investigation was performed using Detector Duo ground penetrating radar, produced by Ingegneria dei Sistemi (IDS). The main characteristics of this system is simultaneous use of two frequencies, allowing the identification of both shallow and deep objects at the same time. Two antennas have frequencies of 700MHz and 250MHz located in a single container. The system is consisted of antenna box, control unit, battery, all mounted on the trolley equipped with position sensor. Control unit is the heart of the system and it communicates with the antennas, notebook PC and pilots position sensor. [17]



Figure (29): Detector Duo GPR device used in acquisition.

Prior to the investigation, GPR usually requires calibration to obtain current parameters of the soil. Calibration can be repeated as often as required, whenever soil conditions change. Also, it is possible to chose to perform scans with or without reference coordinates, choose the option to

save data on external devices, customize gain and filtering, choose measure unit etc. During the acquisition it is possible to see the real time radar map on the PC connected to the central unit, which is automatically gained and filtered (optional). As said previously, the system is equipped with two antennas, and both radar maps are possible to view in real time during the survey. During the survey it is possible to mark in real time encountered objects if one is sure what they represent, and different markers are available. The vertical line on a display permits to track trolley position at any time and position it correctly of one wants to see something specific. [17]

6.2 ACQUISITION

The main aim of the survey was to identify potential remains of old oratorio, ancient road and explore the site in order to find tombs or some other remains. There were no maps found where exact position of the oratorio could be indicated, so the area had to be explored.

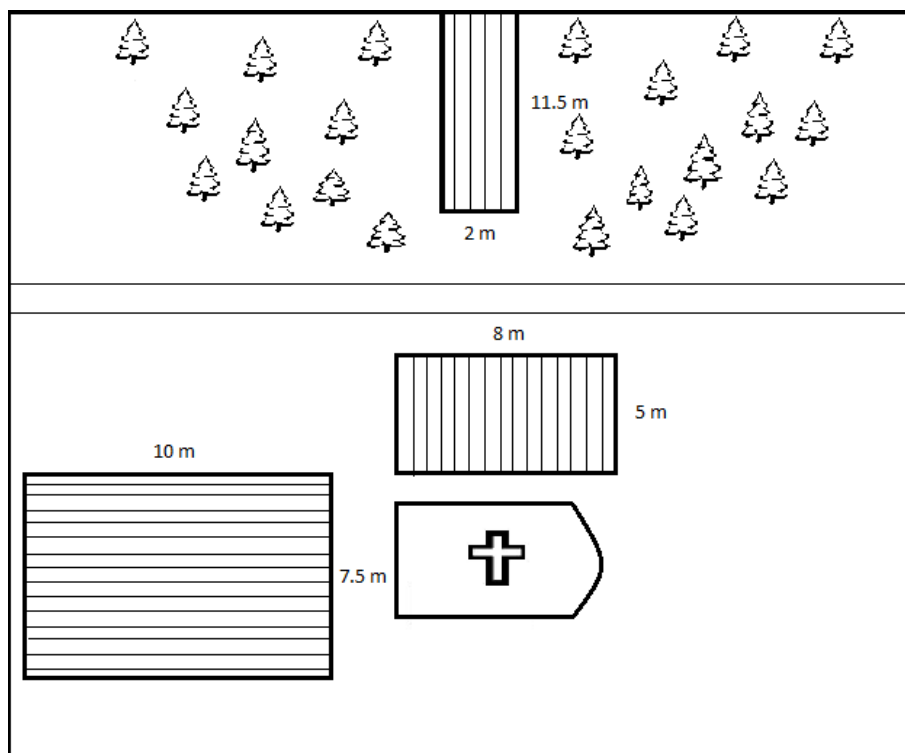


*Figure (30): scheme of micro area of the church with points of interest chosen for survey
(dimensions and line orientation)*

The road was built with the arrival of Romans and division of the area in *centurie*, around 200 ac. On the 1722 map (Figure (28)) it was indicated that the road was passing by the church on its eastern side, but it was not clear how far from the church. As explained in previous chapter, the local population had been taking upper layers from the road to construct the houses once the road lost its significance, so it was assumed that the road might be hard to detect. The last point of interest were eventual tombs and graves, as well as the other possible remains.

In the initial phase of the investigation it was necessary to make a random check on the site to identify points of interest for which data will be collected. During the check, there were found no anomalies that would indicate the presence of foundations or parts of the walls of the oratorio. In this way, the search for oratorio has finished in the very initial phase and it was concluded that it was not built, at least in the close proximity of the church.

Northern side: certain anomalies have been detected on the northern side of the church and it was chosen as a first point of interest. Due to the terrain characteristics it was suspected to be an old cemetery. It was chosen a piece of land 8 x 5 meters, with 0.25 meters separation between the lines. It was decided to make parallel profiles, in direction North-South.



Figure (31): acquisition in progress on the left side and a piece chosen for investigation called “Cemetery”, shown on the right.

Random survey was performed also on the northern side at the entrance to the forest. Strong anomaly was detected and it has been decided to perform an acquisition on one piece, in the direction North-South, 11.5 x 2 meters, with the line separation of 0.5 meters.



Figure (32): a chosen piece for investigation on the entrance of the forest, called “Hill”.

Eastern side: on the eastern side the terrain has been explored searching for the road and a number of anomalies has been detected in close proximity of the church, around 10 meters. The anomalies were detected in most of the parallel lines in the direction West-East and it was assumed that this might be the old road. It was chosen a piece of dimensions 10 x 7.5 meters, with line separation of 0.5 meters.



Figure (33): a piece chosen after random survey where the road is suspected to be.

7. RESULTS AND DISCUSSION

The main aim of the data processing was to provide better understanding of the encountered anomalies. The data have been processed using REFELEX 5.5, mainly following the literature suggestions and the main steps were involving: data editing, basic processing (dewow, filtering, gain) and advanced processing (background subtraction, velocity analysis, static correction, migration, attribute analysis). [6]

During the data editing, mainly file headers were corrected for distances in X and Y direction to allow tridimensional interpretation to compensate for the field errors. Data were dewowed and bandpass filter have been applied. Afterward, gain was applied to the data to try to amplify weaker signals. In some cases energy decay has been used, in other gain function has been applied to the traces. Gaining was followed by background removal and bandapss filtering. Velocity was estimated by using hyperbola fitting, and using the data hyperbolas were collapsed using data migration. Migration was performed in order to recover the true shape of subsurface reflectors. This technique, by collapsing the diffraction hyperbolas due to small-scale heterogeneities, enhances the most significant events. Attribute analysis (envelope) was used as the very last step for better data visualization.

Initially, one sole GPR line is chosen from each of the datasets and processed, with the aim to identify right sequence and parameters of processing steps for all dataset. The sole line was processed using REFLEX 2D module. After identifying right processing steps and parameters, all datasets have been processed in sequence, producing final results which were ready for tridimensional interpretation.

The results of the each individual processing step have been shown bellow. In the processing of the following datasets only key points will be highlighted. Tridimensional interpretation was performed using REFLEX 3D module.

7.1 THE ROAD

As mentioned before, acquisition was performed on a piece with dimensions 10 x 7.5 meters, with 0.5 meter line separation, perpendicular to possible road direction. This separation is considered as maximal possible for good 3D data interpretation. The processing flow is shown bellow in the Figure (34) and has mainly included the steps introduced in the beginning of the chapter. In the first image in Figure (34) it is indicated the area of the profile where the strong anomaly has been detected, probably representing the road.

It was expected to see strong horizontal reflectors but 2D analysis has showed notable differences among the different vertical profiles and only few profiles have showed high contrast reflectors. Having in mind that Roman roads were usually constructed in different layers of stones, gravel and cobbles at the top, this was in contrary with the expectations and may indicate that the cobbles were removed at one point so the road is heavily damaged.

Tridimensional interpretation confirms that it is hard to distinguish the exact position of the road. From the Figure (35) it can be concluded that the possible location of the road could be around 8th meter in x direction, from the 0.3 to 0.5 meters in depth. A number of unknown anomalies is present also from 1st to 5th meter on the depth of around 0.5 meters, but no continuity was noticed. After migration was performed it can be concluded that anomalies could be associated to the stones.

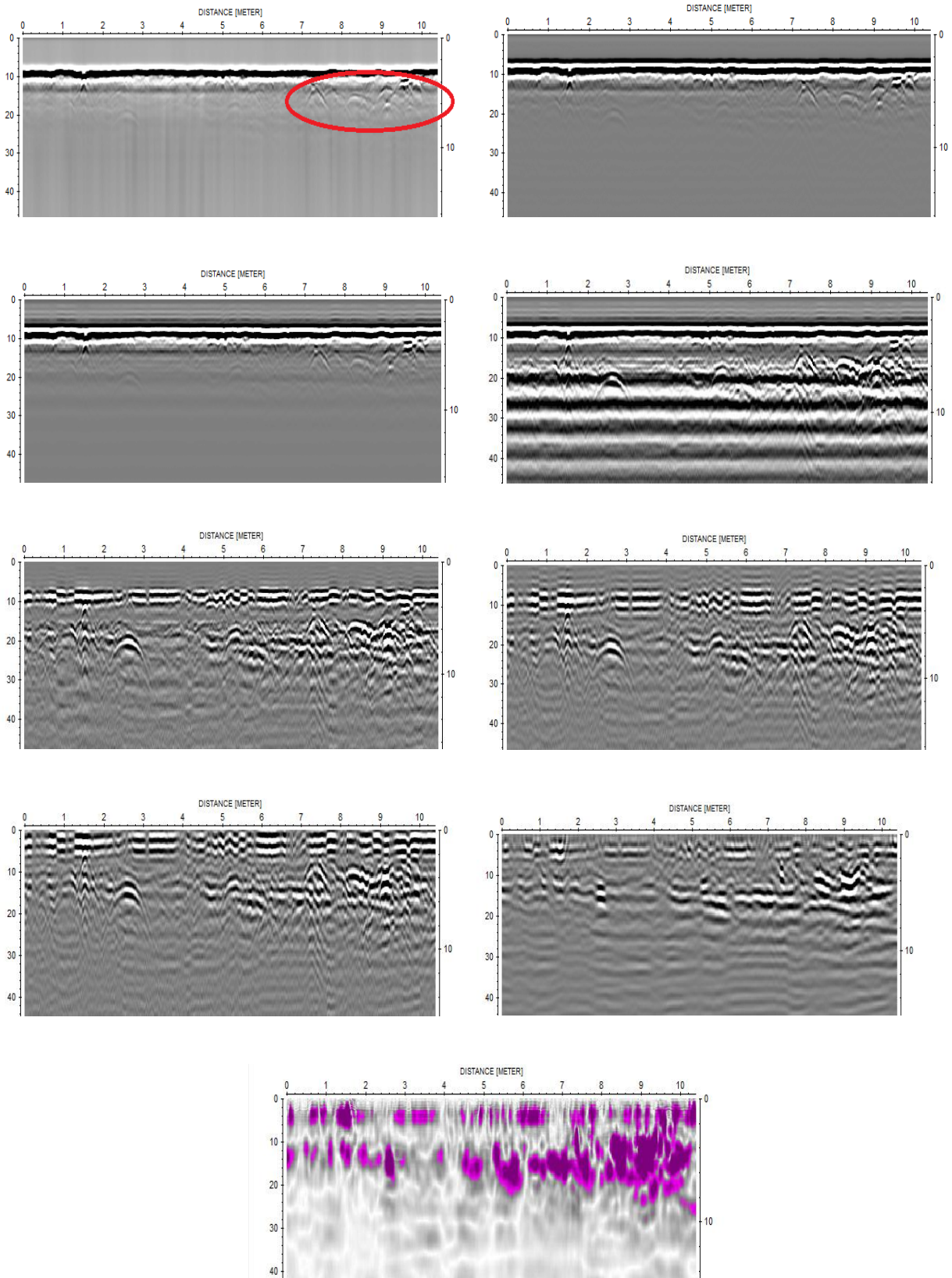


Figure (34): the processing flow of the road dataset, showing in the consecutive order: original profile, dewowed profile, filtered profile, gain applied, background subtraction, filtered, start time moved, migrated profile and profile with envelope applied.

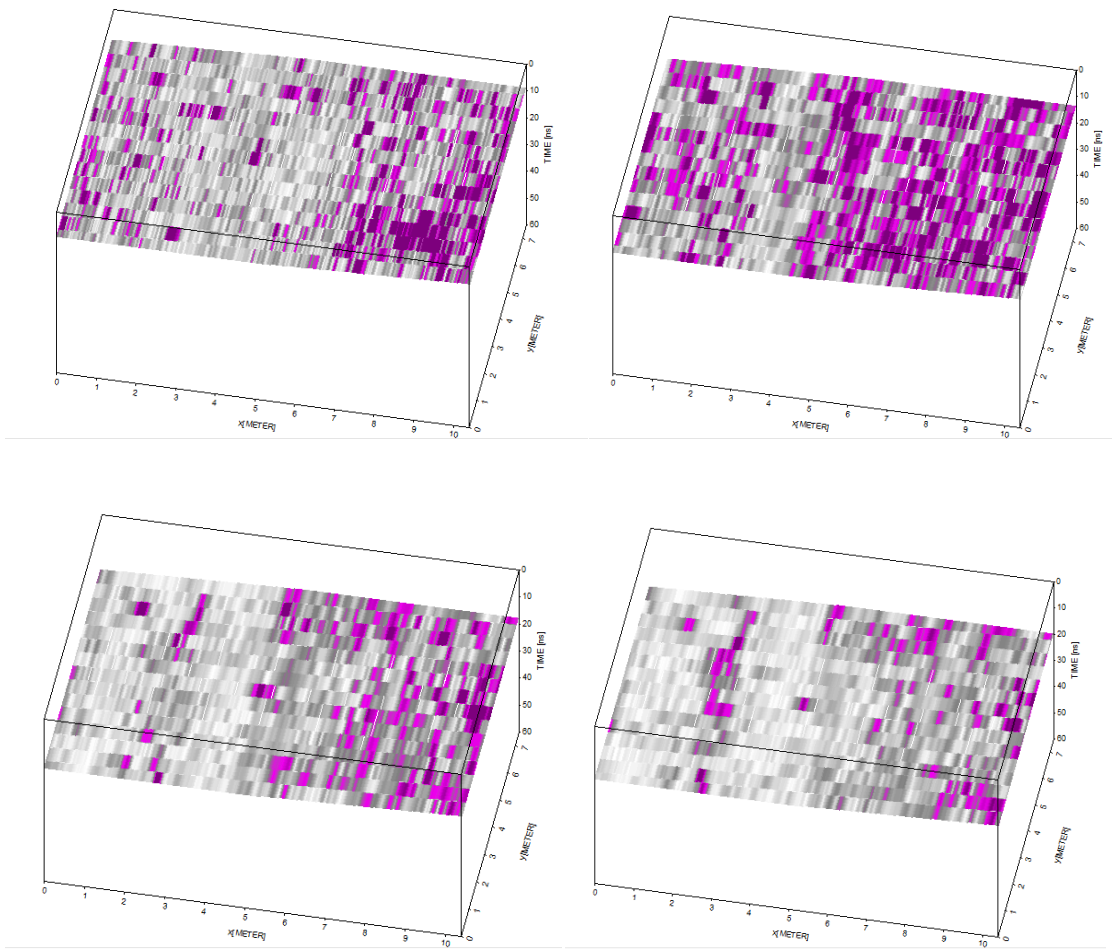


Figure (35): time slices of the 3D interpretation of the dataset taken in consecutive order, from left to right, at: 9 ns (32.5 cm), 15 ns (52.5 cm), 18 ns (56 cm) and 20 ns (70 cm).

7.2 CEMETERY

The dataset has been processed following the steps already described in the beginning of the chapter. In the graveyards, graves are usually placed in order, and detecting such “pattern” is a key element in the research. During 2D analysis certain patterns have been detected (as shown in Figure (36)) on some profiles but after migration has been performed it was discovered that the responses were mainly due to the presence of stones.

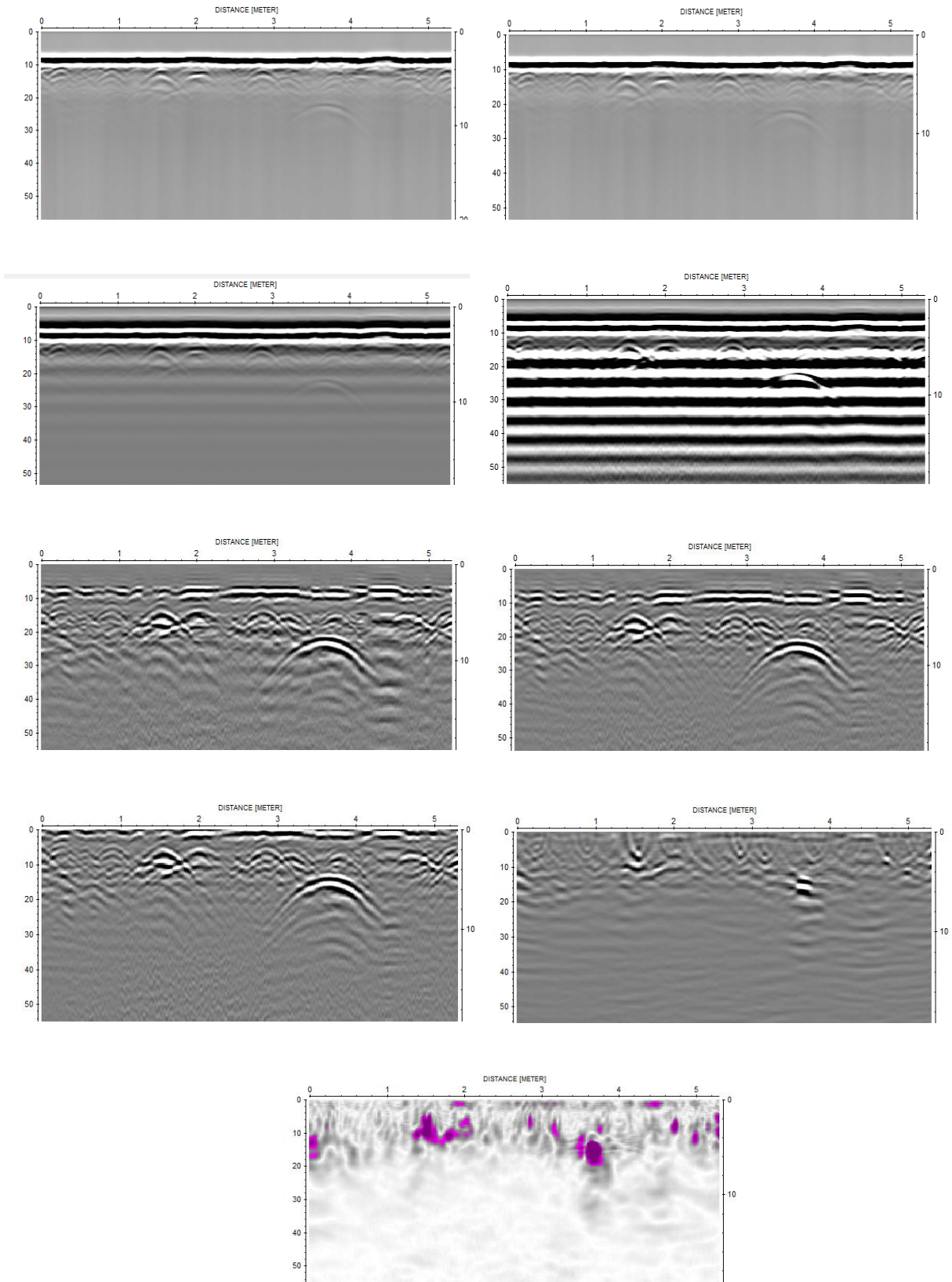


Figure (36): the processing flow of the cemetery dataset, showing in the consecutive order: original profile, dewowed profile, filtered profile, gain applied, background subtraction, filtered, start time moved, migrated profile and profile with envelope applied.

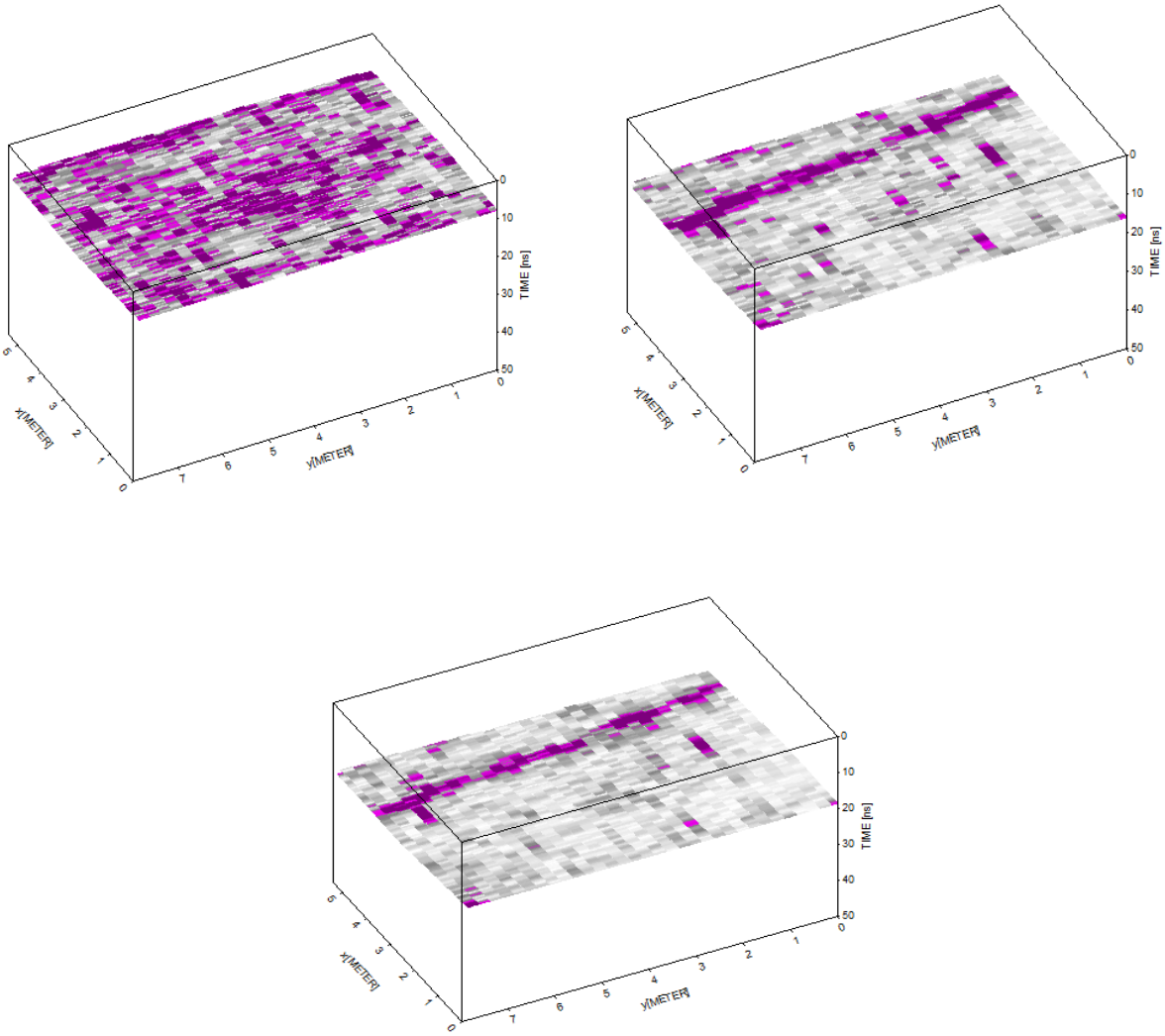


Figure (37): time slices of the 3D interpretation of the dataset taken in consecutive order, from left to right, at: 16 ns (0.28 m), 16 ns (0.64 m) and 19 ns (0.76 m).

Also, 3D interpretation is shown on Figure (37), where it revealed clearly visible metal pipe, located approximately 0.6 meters under the ground. An interesting anomaly has been shown, on 2nd meter in y direction and 3rd meter in x direction. The anomaly could be a larger stone or some other object and it is difficult to speak about possible presence of the grave. It is visible on two profiles, which are shown on a Figure (38) and marked as U. Anomaly on the right side, marked as P represents metallic pipe.

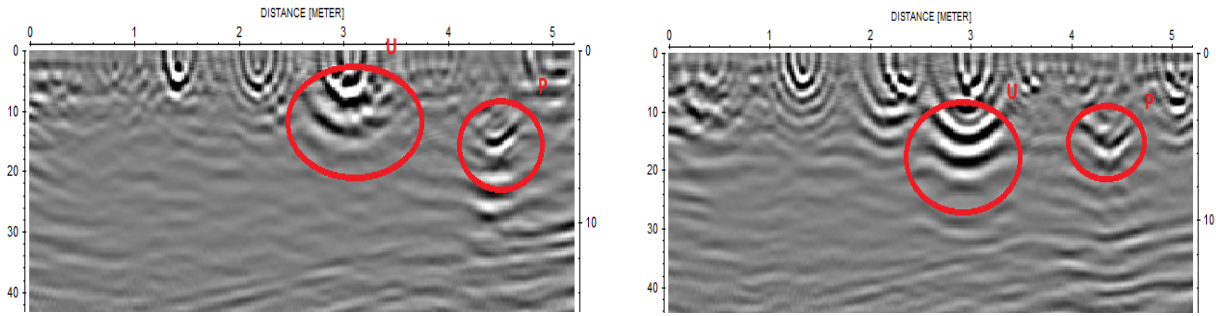


Figure (38): two consecutive profiles, showing pipe marked with P and an anomaly which could be probably associated with large stone.

7.3 THE HILL

The dataset was processed following the order which was presented in the beginning of the chapter. The profiles were very similar, showing mostly roots of the trees in the upper one meter of the profile. In the first meter in X direction (profiles number 4 and 5) on the depth of 2 meters a strong anomaly has been encountered (highlighted in the Figure (39) bellow). By the response it is probably a metallic object. No other interesting anomalies have been detected during the 2D processing.

3D data interpretation has confirmed the results of 2D processing, in the top layers mainly roots are visible and in the middle layer, between 1 m and 2,4 m there are no significant anomalies. At the 2,48 m depth there is a significant unknown anomaly. In the Figures (40) and (41) Y-slices and time slices are shown respectively.

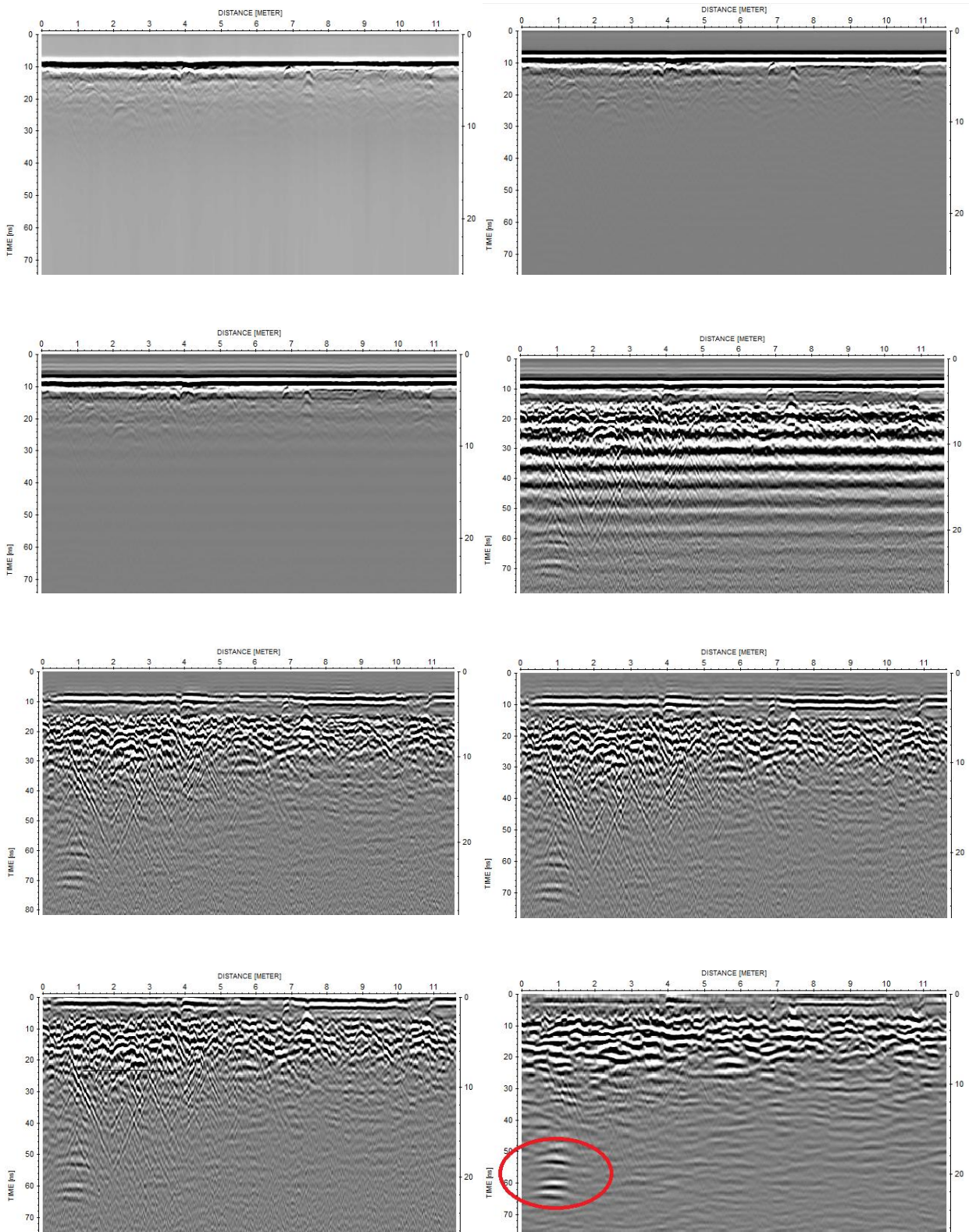


Figure (39): the processing flow of the cemetery dataset, showing in the consecutive order: original profile, dewowed profile, filtered profile, gain applied, background subtraction, filtered, start time moved and migrated profile.

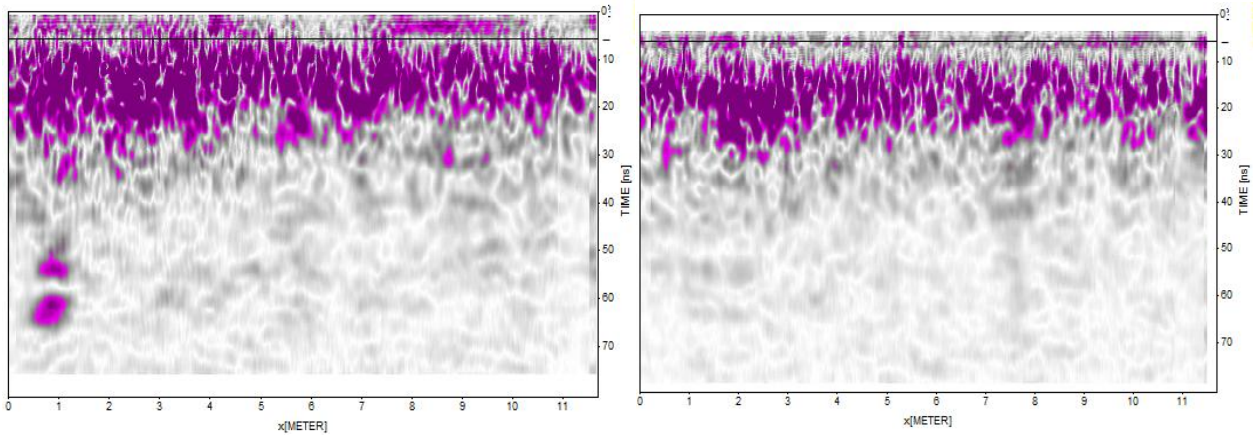


Figure (40): Y-slices of the 3D cube

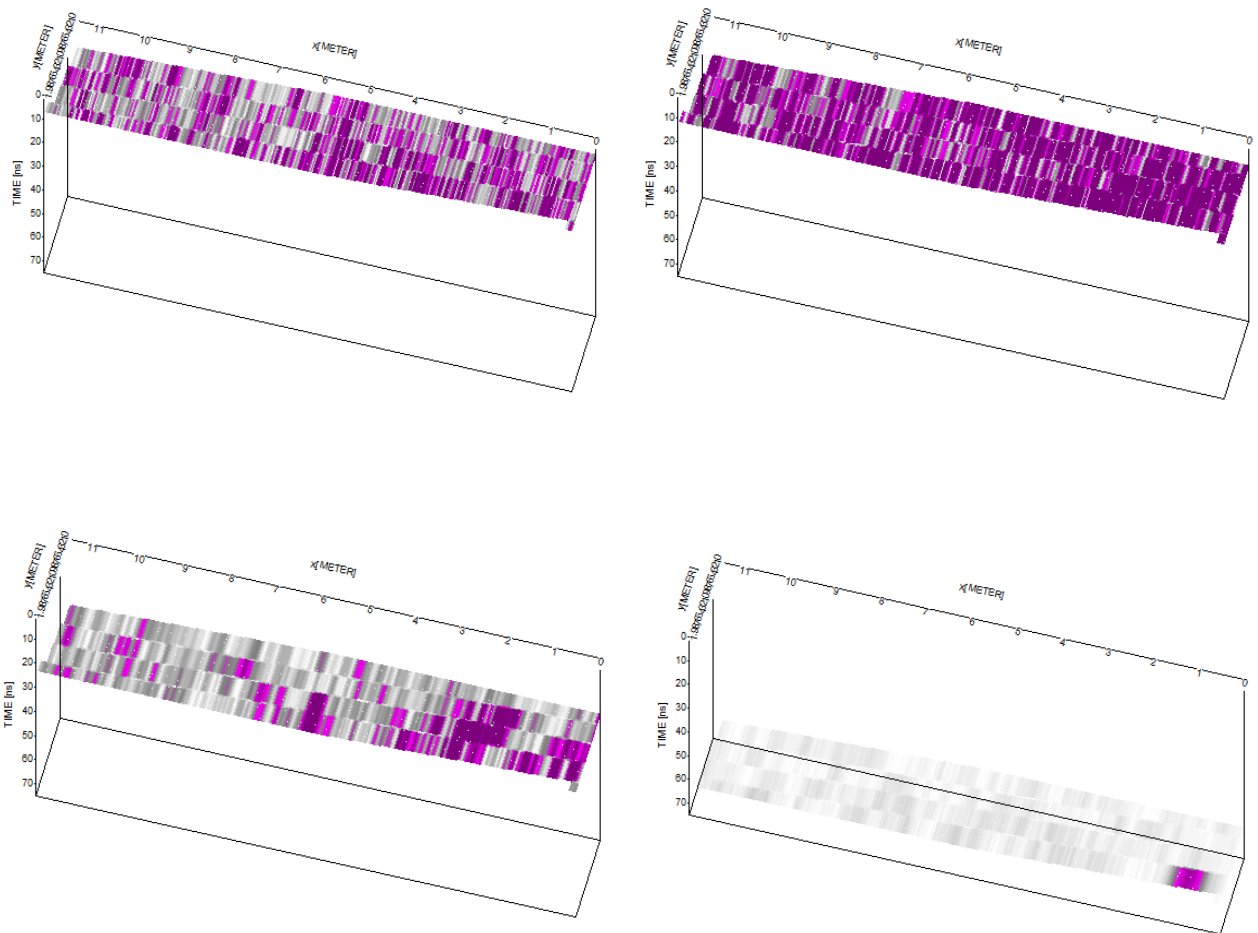


Figure (41): time-slices of the 3D interpretation of the dataset taken in consecutive order, from left to right, at: 7 ns (0.35 m), 15 ns (0.60 m), 23 ns (0.92 m) and 62 ns (2.48 m).

8. CONCLUSIONS AND RECOMMENDATIONS

8.1 CONCLUSIONS

GPR investigation on the site can be regarded as quite successful at capturing archeological features. The penetration of the electromagnetic waves was ranging from 1,5 – 3 meters, which was enough to determine accurate positions of the certain archeological features. In the case of Roman road it was only partially possible to determine its accurate position, due to its condition. Generally, GPR has proved to be good prospection tool for identifying potential area of interest and have manage to provide understanding of the location, especially in the area where there were some historical data.

However, in cases where was lack of historical data it was quite hard to interpret the results. This is due to the ambiguous nature of GPR, where we usually can easily get the answer about the position of the anomaly but not about its nature. In many cases, responses similar to archeological features can be produced also by roots or stones. Data processing and interpretation is very subjective and the processor have to be sincere and provide realistic interpretation. In this case we can speak about GPR ambiguity which is, as we have shown, is very difficult to quantify and will probably be a debate in the close future. Up to now, the only reliable way for verifying GPR results in archeology is excavation.

Understanding local conditions and historical research are proved to be essential for a success of GPR acquisition. This is because the choice of frequency is dependent on the possible depth of the target and at the same time it depends on the local conditions in the subsurface (contrast). It is important to set the acquisition parameters so the GPR electro-magnetic waves are able to penetrate the ground and reach the target. During the acquisition at Saint Adriano church local conditions were good and the contrast between surrounding material and features was enough to generate the response.

8.2 RECOMMENDATIONS

Since it is quite difficult to quantify the uncertainty in GPR acquisition, the processor himself should be honest in giving explanations and present not only his best results but all of them. In this way we cannot speak about definitive interpretations but about relative ones. In this sense we can argue that certain anomaly “might” represent something, but we should not say that it “is” something. This is especially important in case when there is lack of historical data and we cannot make precise interpretation of the anomaly. Another important issue is to have a good experience in dealing with GPR because even the best processed profile will tell nothing to someone who is not familiar with the topic. To be able to claim that we have achieved good results GPR investigation should be accompanied or by extensive historical research or joined with some other geophysical method (such as electrical or gravity measurements) which could provide us better understanding of the anomaly.

TABLE OF FIGURES

Figure (1): approximate rates of change in conductivity.....	19
Figure (2): cone of transmission spreading down the subsurface.....	24
Figure (3): ringing effect created by a reflection from metal object.....	27
Figure (4):parabolic response of point source reflectors, typical for pipes.....	28
Figure (5): the response of planar reflectors.....	28
Figure (6): example of matching a hyperbola to raw field data.....	30
Figure (7): overview of ground penetrating radar (GPR) data processing flow.....	34
Figure (8): A profile before and after application of dewow.....	36
Figure (9): a profile after application of dynamic Automatic Gain Control – AGC.....	37
Figure (10): A profile before and after application of manual SEC gain.....	38
Figure (11): a profile before and after application of a bandpass filter.....	39
Figure (12): a profile before and after application of background subtraction.....	40
Figure (13): a profile before and after deconvolution applied.....	41
Figure (14): a profile before and after migration.....	42
Figure (15): A profile before and after application of envelope.....	44
Figure (16): horizontal normalized radar section 500 MHz antenna.....	48
Figure (17): horizontal normalized radar section done with 500 MHz antenna.....	49
Figure (18): horizontal normalized radar section done with 500 MHz antenna.....	50
Figure (19): the most interesting slice 9 – 14 ns.....	51
Figure (20) : Position of the Roman road and the fault zone near Sultanhisar.....	52
Figure (21): 250 MHz antenna profile of Roman Road.....	53
Figure (22): zoom view of the left part in Figure (21).....	53
Figure (23): zoom view of the left part in Figure (21).....	54
Figure (24): location of Saint Adriano church in Olgelasca, Brenna.....	56

Figure (25): division of the area in centurie.....	57
Figure (26): archeological features found in Roman tomb.....	57
Figure (27): the Roman altar found in Olgelasca.....	58
Figure (28): cadastral map of the area from 1722.....	59
Figure (29): Detector Duo GPR device used in acquisition.....	61
Figure (30): scheme of micro area of the church with points of interest chosen for survey.....	62
Figure (31): acquisition in progress on the left side and a piece chosen for investigation.....	63
Figure (32): a chosen piece for investigation on the entrance of the forest, called “Hill”.....	64
Figure (33): a piece chosen after random survey where the road is suspected to be.....	65
Figure (34): the processing flow of the road dataset.....	68
Figure (35): time slices of the 3D interpretation of the dataset.....	69
Figure (36): the processing flow of the cemetery dataset.....	70
Figure (37): time slices of the 3D interpretation of the dataset taken in consecutive order.....	71
Figure (38): two consecutive profiles, showing pipe marked with P and an anomaly.....	72
Figure (39): the processing flow of the cemetery dataset.....	73
Figure (40): Y-slices of the 3D cube.....	74
Figure (41): time-slices of the 3D interpretation of the dataset.....	74

TABLES

Table (1). Typical values for radar parameters for some common materials.....20

REFERENCES

- [1] Geophysical Archaeology Research Agendas for the Future: Some Ground-penetrating Radar Examples, L. CONYERS, Department of Anthropology, University of Denver, Denver, CO, USA ;
- [2] An Analysis of Ground-Penetrating Radar's Ability to Discover and Map Buried Archaeological Sites in Hawai'i, L. B. Conyers, Department of Anthropology, University of Denver, Hawaiian Archaeology, 2007;
- [3] Ground-penetrating Radar Processing and Interpretation Techniques for Archaeology, L. B. Conyers, Department of Anthropology, University of Denver, Denver, Colorado;
- [4] GPR: Theory and Applications, H.M. Jol, Elsevier 2009;
- [5] The use of GPR for archeology: determining site formation processes and subsurface features on Tutuila island, American Samoa D. R.WELCH, Texas A&M University, 2006;
- [6] Ground Penetrating Radar Theory, Data Collection, Processing, and Interpretation: A Guide for Archaeologists, L. Dojack, 2012;
- [7] Introduction to GPR, L. B. Conyers, Altamira press, 2004;
- [8] An introduction to environmental geophysics, J. M. Reynolds, John Wiley & Sons Inc, New York, USA, 1997;
- [9] Seeing the Unseen: Geophysics and Landscape Archeology, S. Campana, S. Piro, CRC Press, London, UK, 2009;
- [10] GPR Workshop Notes, A. P. Annan, Sensors & Software Inc., Ontario, Canada, 2001;
- [11] Field geophysics, J. Milson, University College London, John Wiley & Sons Inc, New York, 2003;
- [12] GPR: Second Edition, D. J. Daniels, Institution of Electrical Engineers, London, UK, 2004;
- [13] www.wikipedia.org

- [14] Ground Penetrating Radar Fundamentals, J. J. Daniels, Department of Geological Sciences, The Ohio State University,
- [15] Investigation of buried objects with Ground Penetrating Radar: Application to archaeoseismology and palaeoseismology in the Buyuk Menderes Graben (Turkey), C. Ç. Yalçiner, University of Strasburg, 2009;
- [16] Storia di Mariano Comense, Fulvia Butti, 1958;
- [17] Detector Duo system, user manual, Ignegneria dei Sistemi, 2007;
- [18] www.storiadibrenna.it
- [19] A ground-penetrating radar survey for archaeological investigations in an urban area _Lecce, Italy, V. Basile, M.T. Carrozzo, S. Negri, L. Nuzzo, T. Quarta, A.V. Villani, Dipartimento di Scienza dei Materiali,Universita Degli Studi di Lecce, 1999.